

## Chapter 2

# Single-Term and Multi-Term Nonuniform Time-Stepping Approximation Methods for Two-Dimensional Time-Fractional Diffusion-Wave Equation

In this chapter, two efficient schemes are proposed to handle the accuracy near the singularity at  $t = 0$  in solving two-dimensional TFDW equation. For the approximation of the TFCD, we use Nonuniform  $L1$  method (single-step) and Nonuniform Crank-Nicolson  $L1 - 2$  method (multi-step). After that, we adopt these two methods to approximate TFCD and apply the central difference operator for the space direction derivative approximations to get the system of equations for considered model. The ADI approach developed to solve the two-dimensional TFDW equation. Further, the stability analysis of these two schemes are proved. Two numerical

examples are given for 1D and 2D TFDW equation with smooth and non-smooth exact solutions to validated the theoretical findings.

## 2.1 Introduction

In this chapter, we discuss and analyze two difference schemes to solve the following two-dimensional TFDW equation:

$${}^C\mathcal{D}_{0,t}^\alpha u(x, y, t) = u_{xx}(x, y, t) + u_{yy}(x, y, t) + f(x, y, t), \quad (x, y, t) \in \Omega \times (0, T], \quad (2.1)$$

$$u(x, y, t) = \Phi(x, y, t), \quad (x, y, t) \in \partial\Omega \times (0, T], \quad (2.2)$$

$$u(x, y, 0) = \phi(x, y), \quad u_t(x, y, 0) = \varphi(x, y), \quad (x, y) \in \Omega, \quad (2.3)$$

where,  $\Omega = (0, L_1) \times (0, L_2)$  and  $\bar{\Omega} = \Omega \cup \partial\Omega$ , the functions  $\Phi$ ,  $\phi$ ,  $\varphi$  and  $f$  are sufficiently smooth functions. The operator  ${}^C\mathcal{D}_{0,t}^\alpha$  is the TFCD of order  $\alpha$  ( $1 < \alpha < 2$ ), which is defined as:

$${}^C\mathcal{D}_{0,t}^\alpha u(t) = \int_0^t \omega_{2-\alpha}(t-s)u''(s) ds, \quad (2.4)$$

with,  $\omega_\alpha(t) = \frac{t^{\alpha-1}}{\Gamma(\alpha)}$ . Due to the nonlocal property and the history dependence character of the fractional derivatives, it is a difficult task to find the numerical solution of the 2D TFDW equation.

Several research works are available in the literature to handle the initial singularity in TFCD of order  $\beta \in (0, 1)$ . These works showed that the approximation methods have better accuracy on nonuniform meshes [64, 111, 112] as compared to uniform meshes for  $0 < \beta < 1$ . In the literature, the existing numerical methods for solving TFDW equation are done on uniform temporal meshes by taking smooth exact

solution under some restrictive regularity conditions with smooth initial data. However, the solution layer at initial singularity  $t = 0$  for the TFCD of order  $\alpha \in (1, 2)$  remains to be addressed. The main purpose of this chapter is to deal with the initial singularity of the TFCD of order  $\alpha \in (1, 2)$ . To overcome the low accuracy caused by nonsmooth exact solutions of TFDW equation, this chapter includes the discretization of TFCD of order  $\alpha \in (1, 2)$  on nonuniform time mesh. We present two difference schemes with  $(3 - \alpha)$  and second order accuracy in time direction to solve the 1D and 2D TFDW equations.

### **Contribution and purpose of proposed work**

- The proposed work consists of two approximation methods namely  $L1$  (single-term approximation method) and Crank-Nicolson  $L1 - 2$  (multi-term approximation method) on nonuniform temporal grids for the approximation of the TFCD at the grid points  $t = t_n$  and  $t = t_{n-\frac{1}{2}}$ , respectively. We show numerical experiments to test these approximation methods and give graphical representations to analyze the behavior of nonuniform meshes near the singular point  $t = 0$ .
- Adapting these nonuniform approximation methods, we establish two difference schemes using ADI approach for solution of the 2D TFDW equations with weakly singular solutions.
- With some regularity conditions on the solution of the TFDW equation and weak restrictions on mesh points, the Nonuniform  $L1$  difference scheme attains convergence order  $\mathcal{O}(N^{-\gamma(3-\alpha)} + h_1^2 + h_2^2)$  and the Nonuniform Crank-Nicolson  $L1 - 2$  scheme achieve second-order accuracy in both time and space-direction.

- To illustrate the advantage of the nonuniform difference schemes, we present some numerical examples for non-smooth exact solutions with strong singularity at  $t = 0$ .

The outline of the chapter is arranged as follows: In Section 2.2, we discuss two approximation methods namely Nonuniform  $L1$  method and Nonuniform Crank-Nicolson  $L1 - 2$  method to approximate TFCD and prove the local truncation error bounds of these methods. Two difference schemes based on ADI approach for the considered problem (2.1)-(2.3) having singularity at  $t = 0$  in the exact solution are derived in Section 2.3. Stability analysis is discussed for these two difference schemes in Section 2.4. In Section 2.5, we present the fully discrete difference schemes derived in Section 2.3 to solve and validate 1D TFDW equation. We present two numerical examples with smooth and non-smooth exact solutions to verify the theoretical convergence rate in Section 2.6. A brief conclusion of the work is discussed in Section 2.7.

## 2.2 Approximation Methods to Discretize the Time-Fractional Caputo Derivative of Order $\alpha \in$

(1, 2)

Suppose  $0 = t_0 < t_1 < \dots < t_{n-1} < t_n < \dots < t_N = T$  be a nonuniform partition of the time domain  $[0, T]$  with the grid length  $\tau_n = t_n - t_{n-1}$ , ( $1 \leq n \leq N$ ) along the assumption  $\tau_{n-1} \leq \tau_n$ . Throughout the chapter, we use the node points  $t_k = (k\tau)^\gamma$ ,  $0 \leq k \leq n$  for  $\gamma \geq 1$  is a mesh grading parameter, where  $\tau = T^{\frac{1}{\gamma}}/N$ , and  $N$  is the number of subintervals during the partition of domain  $[0, T]$ . Define the fractional time grid points  $t_{n-\theta} = \theta t_{n-1} + (1 - \theta)t_n$ , for any  $\theta \in [0, 1]$ ,  $n \geq 1$  and

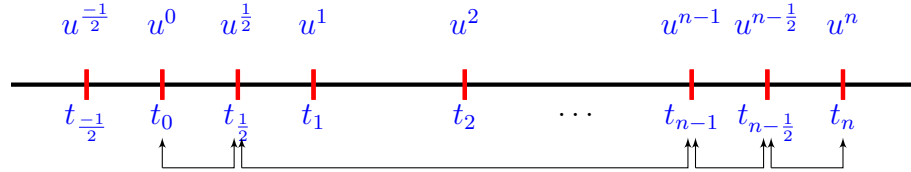
$\mathcal{V} = \{v(t_n) = v^n \mid 1 \leq n \leq N\}$ . For  $v \in \mathcal{V}$ , we introduce the following notations

$$\begin{aligned} v^{n-\frac{1}{2}} &= \frac{v^n + v^{n-1}}{2}, & \delta_t v^{n-\frac{1}{2}} &= \frac{v^n - v^{n-1}}{\tau_n}, \\ \delta_t^2 v^{n-\frac{1}{2}} &= \frac{2}{\tau_n} \left[ \frac{(v^{n+\frac{1}{2}} - v^{n-\frac{1}{2}})}{(\tau_{n+1} + \tau_n)} - \frac{(v^{n-\frac{1}{2}} - v^{n-\frac{3}{2}})}{(\tau_n + \tau_{n-1})} \right]. \end{aligned}$$

Setting  $v(t) = \frac{\partial u}{\partial t}(t)$ , then  $v^{n-\frac{1}{2}} \approx \frac{\partial u}{\partial t}(t)|_{t_{n-\frac{1}{2}}}$ . Now, we present the Nonuniform  $L1$  and Nonuniform Crank-Nicolson  $L1 - 2$  method for approximation of TFCD.

## 2.2.1 Nonuniform $L1$ Method

Let  $v \in C[0, T] \cap C^2(0, T]$  such that  $v = u'$ , then  ${}_0^C D_t^\alpha u(t) = {}_0^C D_t^{\alpha-1} v(t)$ ,  $1 < \alpha < 2$  discussed in [62]. We generalize the discretization idea of TFCD defined in [1] to nonuniform time grids. Now, the discretization of TFCD at the grid point  $t = t_n$  is calculated on the following steps:



$$\begin{aligned} {}_0^C \mathcal{D}_{0,t}^\alpha u(t)|_{t=t_n} &= \sum_{k=0}^{n-1} \int_{t_{k-\frac{1}{2}}}^{t_{k+\frac{1}{2}}} \omega_{2-\alpha}(t_n - s) v'(s) ds - \int_{t_{-\frac{1}{2}}}^{t_0} \omega_{2-\alpha}(t_n - s) v'(s) ds \\ &\quad + \int_{t_{n-\frac{1}{2}}}^{t_n} \omega_{2-\alpha}(t_n - s) v'(s) ds. \end{aligned} \quad (2.5)$$

- Linear interpolation polynomial on the first integration of the equation (2.5) using  $(t_{k-\frac{1}{2}}, v^{k-\frac{1}{2}})$ ,  $(t_{k+\frac{1}{2}}, v^{k+\frac{1}{2}})$ ,  $(0 \leq k \leq n-1)$  and let,  $t_{-\frac{1}{2}} = t_0$ .

- Linear interpolation polynomial on the last integration of the equation (2.5) using  $(t_{n-\frac{3}{2}}, v^{n-\frac{3}{2}})$ ,  $(t_{n-\frac{1}{2}}, v^{n-\frac{1}{2}})$ ,  $n \geq 1$  and let,  $t_{-\frac{1}{2}} = t_0$ . Then, we have

$$v(t_{-\frac{1}{2}}) = \frac{\partial u(t)}{\partial t} \Big|_{t_{-\frac{1}{2}}} + \mathcal{O}(\tau_n^2) \implies \frac{u(t_0) - u(t_{-1})}{t_0 - t_{-1}} = v(t_0) + \mathcal{O}(\tau_n^2). \quad (2.6)$$

Now,

$$\begin{aligned} & {}^C \mathcal{D}_{0,t}^\alpha u(t) \Big|_{t=t_n} \\ &= \sum_{k=0}^{n-1} \left\{ \frac{2}{(\tau_k + \tau_{k+1})} (v^{k+\frac{1}{2}} - v^{k-\frac{1}{2}}) \int_{t_{k-\frac{1}{2}}}^{t_{k+\frac{1}{2}}} \omega_{2-\alpha}(t_n - s) ds \right\} + (\mathcal{R}_1)_t^n \\ &+ \frac{2}{(\tau_{n-1} + \tau_n)} (v^{n-\frac{1}{2}} - v^{n-\frac{3}{2}}) \int_{t_{n-\frac{1}{2}}}^{t_n} \omega_{2-\alpha}(t_n - s) ds + (\mathcal{R}_2)_t^n, \\ &= \sum_{k=0}^{n-1} \left[ \frac{2}{(\tau_k + \tau_{k+1})} \left\{ \frac{(u^{k+1} - u^k)}{\tau_{k+1}} - \frac{(u^k - u^{k-1})}{\tau_k} \right\} \int_{t_{k-\frac{1}{2}}}^{t_{k+\frac{1}{2}}} \omega_{2-\alpha}(t_n - s) ds \right] \\ &+ \frac{2}{(\tau_{n-1} + \tau_n)} \left\{ \frac{(u^n - u^{n-1})}{\tau_n} - \frac{(u^{n-1} - u^{n-2})}{\tau_{n-1}} \right\} \int_{t_{n-\frac{1}{2}}}^{t_n} \omega_{2-\alpha}(t_n - s) ds + (\mathfrak{R})_t^n, \\ &= \frac{2}{\Gamma(3-\alpha)} \left[ \sum_{k=0}^{n-1} \frac{[(t_n - t_{k-\frac{1}{2}})^{2-\alpha} - (t_n - t_{k+\frac{1}{2}})^{2-\alpha}]}{(\tau_k + \tau_{k+1})} \left\{ \frac{(u^{k+1} - u^k)}{\tau_{k+1}} - \frac{(u^k - u^{k-1})}{\tau_k} \right\} \right] \\ &+ \frac{1}{(\tau_{n-1} + \tau_n)} \left( \frac{\tau_n}{2} \right)^{2-\alpha} \left\{ \frac{(u^n - u^{n-1})}{\tau_n} - \frac{(u^{n-1} - u^{n-2})}{\tau_{n-1}} \right\} + (\mathfrak{R})_t^n, \\ &= \sum_{k=0}^{n-1} a_{n-k}^{(n)} \left\{ \frac{(u^{k+1} - u^k)}{\tau_{k+1}} - \frac{(u^k - u^{k-1})}{\tau_k} \right\} \\ &+ \frac{2^{\alpha-1}}{\Gamma(3-\alpha)} \frac{\tau_n^{2-\alpha}}{(\tau_{n-1} + \tau_n)} \left\{ \frac{(u^n - u^{n-1})}{\tau_n} - \frac{(u^{n-1} - u^{n-2})}{\tau_{n-1}} \right\} + (\mathfrak{R})_t^n, \quad (2.7) \end{aligned}$$

where,

$$a_{n-k}^{(n)} := \frac{\int_{t_{k-\frac{1}{2}}}^{t_{k+\frac{1}{2}}} \omega_{2-\alpha}(t_n - s) ds}{t_{k+\frac{1}{2}} - t_{k-\frac{1}{2}}} = \frac{2}{\Gamma(3-\alpha)} \frac{[(t_n - t_{k-\frac{1}{2}})^{2-\alpha} - (t_n - t_{k+\frac{1}{2}})^{2-\alpha}]}{(\tau_k + \tau_{k+1})}, \quad n \geq 1. \quad (2.8)$$

where,  $(\mathfrak{R})_t^n = (\mathcal{R}_1)_t^n + (\mathcal{R}_2)_t^n$ .

**(R1)** For  $1 < \alpha < 2$ ,  $u \in C^2[0, T] \cap C^3(0, T]$ . Then the error on each subintervals are defined as:

$$(\mathcal{R}_1)_t^n = \sum_{k=0}^{n-1} \int_{t_{k-\frac{1}{2}}}^{t_{k+\frac{1}{2}}} \omega_{2-\alpha}(t_n - s) \left\{ v'(s) - \frac{v^{k+\frac{1}{2}} - v^{k-\frac{1}{2}}}{t_{k+\frac{1}{2}} - t_{k-\frac{1}{2}}} \right\} ds, \quad (2.9)$$

$$(\mathcal{R}_2)_t^n = \int_{t_{n-\frac{1}{2}}}^{t_n} \omega_{2-\alpha}(t_n - s) \left\{ v'(s) - \frac{v^{n-\frac{1}{2}} - v^{n-\frac{3}{2}}}{t_{n-\frac{1}{2}} - t_{n-\frac{3}{2}}} \right\} ds. \quad (2.10)$$

Using Taylor theorem for  $v(t)$ ,  $t_{k-\frac{1}{2}} < t < t_{k+\frac{1}{2}}$  with integral remainder, we obtain

$$v'(t) - \frac{v^{k+\frac{1}{2}} - v^{k-\frac{1}{2}}}{t_{k+\frac{1}{2}} - t_{k-\frac{1}{2}}} = \frac{2}{(\tau_{k+1} + \tau_k)} \left[ \int_{t_{k-\frac{1}{2}}}^t (\zeta - t_{k-\frac{1}{2}}) v''(\zeta) d\zeta - \int_t^{t_{k+\frac{1}{2}}} (t_{k+\frac{1}{2}} - \zeta) v''(\zeta) d\zeta \right]. \quad (2.11)$$

From equations (2.9) and (2.11), we get

$$\begin{aligned} (\mathcal{R}_1)_t^n &= \frac{1}{\Gamma(2-\alpha)} \left\{ \sum_{k=0}^{n-1} \frac{2}{(\tau_{k+1} + \tau_k)} \int_{t_{k-\frac{1}{2}}}^{t_{k+\frac{1}{2}}} \left[ \int_{t_{k-\frac{1}{2}}}^s (\zeta - t_{k-\frac{1}{2}}) v''(\zeta) d\zeta \right. \right. \\ &\quad \left. \left. - \int_s^{t_{k+\frac{1}{2}}} (t_{k+\frac{1}{2}} - \zeta) v''(\zeta) d\zeta \right] (t_n - s)^{1-\alpha} ds \right\}, \\ &= \frac{1}{\Gamma(2-\alpha)} \left\{ \sum_{k=0}^{n-1} \frac{2}{(\tau_{k+1} + \tau_k)} \int_{t_{k-\frac{1}{2}}}^{t_{k+\frac{1}{2}}} \left[ \left( \int_{\zeta}^{t_{k+\frac{1}{2}}} (t_n - s)^{1-\alpha} ds \right) (\zeta - t_{k-\frac{1}{2}}) \right. \right. \\ &\quad \left. \left. - \left( \int_{t_{k-\frac{1}{2}}}^{\zeta} (t_n - s)^{1-\alpha} ds \right) (t_{k+\frac{1}{2}} - \zeta) \right] v''(\zeta) d\zeta \right\}, \\ &= \frac{1}{\Gamma(3-\alpha)} \sum_{k=0}^{n-1} \frac{2}{(\tau_{k+1} + \tau_k)} \int_{t_{k-\frac{1}{2}}}^{t_{k+\frac{1}{2}}} \left[ (\zeta - t_{k-\frac{1}{2}}) \{ (t_n - \zeta)^{2-\alpha} - (t_n - t_{k+\frac{1}{2}})^{2-\alpha} \} \right. \\ &\quad \left. - (t_{k+\frac{1}{2}} - \zeta) \{ (t_n - t_{k-\frac{1}{2}})^{2-\alpha} - (t_n - \zeta)^{2-\alpha} \} \right] v''(\zeta) d\zeta, \\ &\leq \frac{1}{\Gamma(3-\alpha)} \sum_{k=0}^{n-1} \left[ \frac{(t_n - t_{k-\frac{1}{2}})^{3-\alpha} - (t_n - t_{k+\frac{1}{2}})^{3-\alpha}}{(3-\alpha)} \right. \\ &\quad \left. - \frac{(\tau_{k+1} + \tau_k)}{4} \{ (t_n - t_{k-\frac{1}{2}})^{2-\alpha} + (t_n - t_{k+\frac{1}{2}})^{2-\alpha} \} \right] \max_{t_0 \leq \eta \leq t_n} |v''(\eta)|, \end{aligned}$$

$$\leq \frac{1}{\Gamma(3-\alpha)} \sum_{k=0}^{n-1} \left\{ \frac{[(2t_n - t_{k-1} - t_k)^{3-\alpha} - (2t_n - t_k - t_{k+1})^{3-\alpha}]}{2^{3-\alpha} (3-\alpha)} - \frac{(\tau_{k+1} + \tau_k)}{4} \right. \\ \left. \frac{[(2t_n - t_{k-1} - t_k)^{2-\alpha} + (2t_n - t_k - t_{k+1})^{2-\alpha}]}{2^{2-\alpha}} \right\} \max_{t_0 \leq \eta \leq t_n} |v''(\eta)|. \quad (2.12)$$

To demonstrate the error bound, the following inequality will be useful.

$$\tau_n := T \left[ \left( \frac{n}{N} \right)^\gamma - \left( \frac{n-1}{N} \right)^\gamma \right] = TN^{-\gamma} [n^\gamma - (n-1)^\gamma], \\ = TN^{-\gamma} n^\gamma [1 - (1 - 1/n)^\gamma] \leq CTN^{-\gamma} n^{\gamma-1}. \quad (2.13)$$

Since  $t_n - t_k = \tau_n + \tau_{n-1} + \dots + \tau_{k+1} = \frac{(\tau_n + \tau_{k+1})}{2}(n-k)$ , therefore

$$(2t_n - t_{k+1} - t_k)^{3-\alpha} = \left[ \frac{\tau_n + \tau_{k+2}}{2}(n-k-1) + \frac{\tau_n + \tau_{k+1}}{2}(n-k) \right]^{3-\alpha} \\ \leq \tau_n^{2-\nu_1} [2(n-k) - 1]^{3-\alpha}. \quad (2.14)$$

By using (2.13), we obtain

$$(2t_n - t_{k+1} - t_k)^{3-\alpha} \leq CN^{-\gamma(3-\alpha)} n^{\{(\gamma-1)(3-\alpha)\}} T^{3-\alpha} [2(n-k) - 1]^{3-\alpha}.$$

Then, bound for first term of summation in (2.12) is

$$\left| (2t_n - t_{k+1} - t_k)^{3-\alpha} - (2t_n - t_k - t_{k-1})^{3-\alpha} \right| \\ \leq (2t_n - t_{k+1} - t_k)^{3-\alpha} + (2t_n - t_k - t_{k-1})^{3-\alpha}, \\ \leq CN^{-\gamma(3-\alpha)} n^{\{(\gamma-1)(3-\alpha)\}} T^{3-\alpha} \{ [2(n-k) - 1]^{3-\alpha} + [2(n-k) + 1]^{3-\alpha} \}, \quad (2.15)$$

and second term bound of (2.12) is:

$$\left| (2t_n - t_{k-1} - t_k)^{2-\alpha} + (2t_n - t_k - t_{k+1})^{2-\alpha} \right| \\ \leq CN^{-\gamma(2-\alpha)} n^{\{(\gamma-1)(2-\alpha)\}} T^{2-\alpha} \{ [2(n-k) + 1]^{2-\alpha} + [2(n-k) - 1]^{2-\alpha} \}, \quad (2.16)$$

By using (2.15) and (2.16) in (2.12). We obtain

$$|(\mathcal{R}_1)_t^n| \leq \widehat{C} \max_{t_0 \leq \eta \leq t_n} |v''(\eta)| N^{-\gamma(3-\alpha)} T^{3-\alpha}. \quad (2.17)$$

Now, equation (2.10) implies that

$$\begin{aligned} & (\mathcal{R}_2)_t^n \\ & \leq \frac{1}{\Gamma(2-\alpha)} \frac{1}{(\tau_n + \tau_{n-1})} \left[ \int_{t_{n-\frac{1}{2}}}^{t_n} (s - t_{n-\frac{3}{2}})(s - t_{n-\frac{1}{2}})(t_n - s)^{1-\alpha} ds \right] \max_{t_0 \leq \hat{\eta} \leq t_n} |v''(\hat{\eta})|, \\ & \leq \frac{1}{\Gamma(4-\alpha)} \left[ \frac{(t_n - t_{n-\frac{1}{2}})^{3-\alpha}}{2} + \frac{2}{(4-\alpha)} \frac{(t_n - t_{n-\frac{1}{2}})^{4-\alpha}}{(\tau_n + \tau_{n-1})} \right] \max_{t_0 \leq \hat{\eta} \leq t_n} |v''(\hat{\eta})|, \\ & \leq \frac{(6-\alpha)}{2^{4-\alpha} \Gamma(5-\alpha)} (\tau_n)^{3-\alpha} \max_{t_0 \leq \hat{\eta} \leq t_n} |v''(\hat{\eta})|, \\ & \leq \frac{(6-\alpha)}{2^{4-\alpha} \Gamma(5-\alpha)} \left(\frac{n}{N}\right)^{\gamma(3-\alpha)} \max_{t_0 \leq \hat{\eta} \leq t_n} |v''(\hat{\eta})| T^{3-\alpha}. \end{aligned} \quad (2.18)$$

We show the behavior of nonuniform meshes in Figure 2.1 when the solution function  $u$  is non-smooth and fails to achieve the optimal OC near the initial singular point  $t = 0$ . In resolving such type of singularities in solution, we employ the nonuniform mesh to recover an optimal OC. The nonuniform meshes assemble the time grids near the singularity for the large value of  $\gamma$ . The time grids become concentrated more speedily near  $t = 0$ . We tested the approximation method derived in (2.35)-(2.40) for  $u(t) = t^2$  and plot the absolute error for different values of  $\gamma$ . We see that the error is decreasing for higher values of  $\gamma$ , also it gets more concentrated near  $t = 0$  for  $\gamma = 5$  as compare to  $\gamma \leq 4$ .

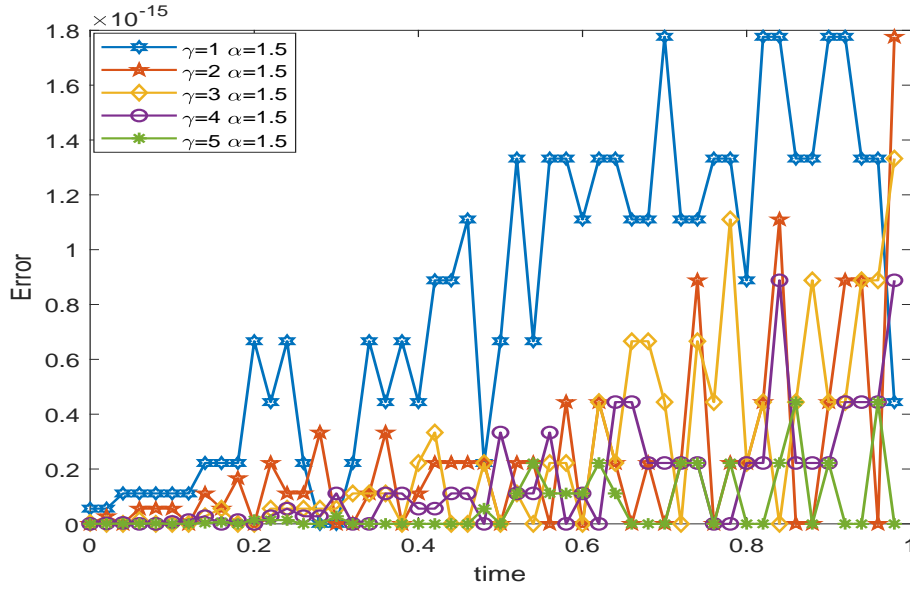


FIGURE 2.1: Error plot for the approximation of  $u(t) = t^2$  using scheme (2.35)-(2.40) with graded meshes and  $N = 50$ .

*Lemma 2.2.1.* For  $1 < \alpha < 2$ , and  $n \geq 1$ , the coefficients  $a_{n-k}^{(n)}$  defined in (2.8) satisfies

$$0 < a_{n-k+1}^{(n)} < a_{n-k}^{(n)}, \quad 1 \leq k \leq n. \quad (2.19)$$

*Proof.* Taking,

$$\frac{2}{(\tau_k + \tau_{k+1})} \int_{t_{k-\frac{1}{2}}}^{t_{k+\frac{1}{2}}} (t_n - \zeta)^{1-\alpha} d\zeta = (t_n - \theta_k)^{1-\alpha}, \quad \theta_k \in (t_{k-\frac{1}{2}}, t_{k+\frac{1}{2}}),$$

and  $(t_n - \zeta)^{1-\alpha}$  is monotonic increasing, we get the result easily.  $\square$

### 2.2.2 Nonuniform Crank-Nicolson $L1 - 2$ Method

To discretize the TFCD of order  $\alpha$  ( $1 < \alpha < 2$ ) at the grid point  $t = t_{n-\frac{1}{2}}$ , we introduce a second-order Nonuniform Crank-Nicolson  $L1 - 2$  scheme. For the approximation of  $u'' = v'$  in equation (2.4), we choose linear interpolation  $\Pi_{1,1}v(t)$  on interval  $[t_0, t_1]$  and quadratic interpolation  $\Pi_{2,k}v(t)$  on other subintervals using points  $(t_{k-2}, v^{k-2})$ ,  $(t_{k-1}, v^{k-1})$ , and  $(t_k, v^k)$ . Suppose  $\widehat{\rho}_k = \frac{\tau_{k-1}}{\tau_k}$ ,  $k \geq 2$ , then applying Newton interpolation polynomials, we get

$$\begin{cases} (\Pi_{1,1}v)'(t) = \frac{v^k - v^{k-1}}{\tau_k}, \\ (\Pi_{2,k}v)'(t) = \frac{v^k - v^{k-1}}{\tau_k} + \frac{2}{\tau_{k-1}(\tau_k + \tau_{k-1})} (t - t_{k-\frac{1}{2}}) [\widehat{\rho}_k (v^k - v^{k-1}) - (v^{k-1} - v^{k-2})]. \end{cases} \quad (2.20)$$

Using the theory of linear interpolation, there exist  $\eta \in (t_0, t_1)$ ,  $\tilde{\eta} \in (t_{k-1}, t_k)$ , we have

$$\begin{cases} v(s) - \Pi_1 v(s) = \frac{1}{2!} v''(\eta) (s - t_0) (s - t_1) \\ v(s) - \Pi_{2,k} v(s) = \frac{1}{3!} v'''(\tilde{\eta}) (s - t_{k-2}) (s - t_{k-1}) (s - t_k), \quad 2 \leq k \leq n. \end{cases} \quad (2.21)$$

Now, the discretization of the TFCD at grid point  $t_n$  is:

$$\begin{aligned} {}^C \mathcal{D}_{0,t}^\alpha u(t_n) &= \sum_{k=1}^n \int_{t_{k-1}}^{t_k} \omega_{2-\alpha}(t_n - s) v'(s) ds \\ &= \int_{t_0}^{t_1} \omega_{2-\alpha}(t_n - s) (\Pi_{1,1}v)'(s) ds + \sum_{k=2}^n \int_{t_{k-1}}^{t_k} \omega_{2-\alpha}(t_n - s) (\Pi_{2,k}v)'(s) ds + r^n, \\ &= d_{n-1}^{(n)} (v^1 - v^0) + \sum_{k=2}^{n-1} d_{n-k}^{(n)} (v^k - v^{k-1}) + d_0^{(n)} (v^n - v^{n-1}) + r^n, \\ &= d_0^{(n)} v^n - \sum_{k=1}^{n-1} (d_{n-k-1}^{(n)} - d_{n-k}^{(n)}) v^k - d_{n-1}^{(n)} v^0 + r^n. \end{aligned} \quad (2.22)$$

This is the compact form of the TFCD discretization. The corresponding coefficients of equation (2.22) are defined as:

For,  $n = 1 \Rightarrow d_0^{(n)} = b_0^{(n)}$ , and for  $n \geq 2$ ,

$$d_{n-k}^{(n)} = \begin{cases} b_{n-1}^{(n)} - c_{n-2}^{(n)}, & k = 1, \\ b_{n-k}^{(n)} + \widehat{\rho}_k c_{n-k}^{(n)} - c_{n-k-1}^{(n)}, & 2 \leq k \leq n-1, \\ b_0^{(n)} + \widehat{\rho}_n c_0^{(n)}, & k = n. \end{cases} \quad (2.23)$$

And, coefficients appeared in the equation (2.23) are defined by

$$\begin{aligned} b_{n-k}^{(n)} &= \frac{1}{\tau_k} \int_{t_{k-1}}^{t_k} \omega_{2-\alpha}(t_n - s) ds \\ &= \frac{1}{\Gamma(3-\alpha)} \left[ \frac{(t_n - t_{k-1})^{2-\alpha} - (t_n - t_k)^{2-\alpha}}{\tau_k} \right], \quad (1 \leq k \leq n) \end{aligned} \quad (2.24)$$

$$c_{n-k}^{(n)} = \frac{2}{\tau_{k-1}(\tau_k + \tau_{k-1})} \int_{t_{k-1}}^{t_k} (s - t_{k-\frac{1}{2}}) \omega_{2-\alpha}(t_n - s) ds, \quad (n \geq 2, 2 \leq k \leq n). \quad (2.25)$$

If  $0 \leq t < t_n$ , then  $\omega_{2-\alpha}(t_n - t) > 0$  and also  $\omega'_{2-\alpha}(t_n - t) > 0, \forall \alpha \in (1, 2)$ . Then, we can rewrite an alternate form for the coefficient  $c_{n-k}^{(n)}$  using integration by parts and Lagrange interpolation theorem as

$$\begin{aligned} c_{n-k}^{(n)} &= \frac{-2}{\tau_{k-1}(\tau_k + \tau_{k-1})} \int_{t_{k-1}}^{t_k} \omega'_{3-\alpha}(t_n - s) ds, \\ &= \frac{1}{\tau_{k-1}(\tau_k + \tau_{k-1})} \int_{t_{k-1}}^{t_k} (t_k - s)(s - t_{k-1}) \omega_{1-\alpha}(t_n - s) ds. \end{aligned} \quad (2.26)$$

Here, we use the Crank-Nicolson method on nonuniform meshes to discretize TFCD at grid point  $t_{n-\frac{1}{2}}$  (see [63]), for  $n \geq 3$ , and obtain the following scheme using (2.22)

$$\begin{aligned} {}^C \mathcal{D}_{0,t}^\alpha u(t_{n-\frac{1}{2}}) &= \frac{{}^C \mathcal{D}_{0,t}^\alpha u(t_{n-1}) + {}^C \mathcal{D}_{0,t}^\alpha u(t_n)}{2}, \\ &= d_0^{(n)} \frac{(v^n + v^{n-1})}{2} - \sum_{k=1}^{n-1} (d_{n-k-1}^{(n)} - d_{n-k}^{(n)}) \frac{(v^k + v^{k-1})}{2} - d_{n-1}^{(n)} v^0 + r^{n-\frac{1}{2}}, \end{aligned}$$

$$= d_0^{(n)} v^{n-\frac{1}{2}} - \sum_{k=1}^{n-1} (d_{n-k-1}^{(n)} - d_{n-k}^{(n)}) v^{k-\frac{1}{2}} - d_{n-1}^{(n)} v^0 + r^{n-\frac{1}{2}}, \quad n \geq 3. \quad (2.27)$$

*Lemma 2.2.2.* Suppose  $g \in C^3[0, T]$ , then

$$\frac{dg}{dt}(t_{k-\frac{1}{2}}) = \frac{g_k - g_{k-1}}{\tau_k} + \mathcal{O}(T^2), \quad k \geq 1. \quad (2.28)$$

*Proof.* Using Taylor's expansion of  $g$  around the node point  $t_{k-\frac{1}{2}}$  on the interval  $[t_{k-1}, t_k]$ , we have

$$\begin{aligned} g(t_{k-1}) &= g(t_{k-\frac{1}{2}}) + (t_{k-1} - t_{k-\frac{1}{2}})g^{(1)}(t_{k-\frac{1}{2}}) + \frac{(t_{k-1} - t_{k-\frac{1}{2}})^2}{2!}g^{(2)}(t_{k-\frac{1}{2}}) \\ &\quad + \frac{(t_{k-1} - t_{k-\frac{1}{2}})^3}{3!}g^{(3)}(t_{k-\frac{1}{2}}) + \dots \\ g(t_k) &= g(t_{k-\frac{1}{2}}) + (t_k - t_{k-\frac{1}{2}})g^{(1)}(t_{k-\frac{1}{2}}) + \frac{(t_k - t_{k-\frac{1}{2}})^2}{2!}g^{(2)}(t_{k-\frac{1}{2}}) \\ &\quad + \frac{(t_k - t_{k-\frac{1}{2}})^3}{3!}g^{(3)}(t_{k-\frac{1}{2}}) + \dots, \end{aligned} \quad (2.29)$$

$$(2.30)$$

using the above equations (2.29) and (2.30), we have

$$\begin{aligned} g^{(1)}(t_{k-\frac{1}{2}}) &= \frac{g_k - g_{k-1}}{t_k - t_{k-1}} + \frac{[(t_k - t_{k-\frac{1}{2}})^3 - (t_{k-1} - t_{k-\frac{1}{2}})^3]}{6(t_k - t_{k-1})}g^{(3)}(t_{k-\frac{1}{2}}) + \dots, \\ &= \frac{g_k - g_{k-1}}{\tau_k} + \frac{\tau_k^2}{24}g^{(3)}(t_{k-\frac{1}{2}}) + \dots \end{aligned} \quad (2.31)$$

Since  $\tau_k = (\frac{k}{N})^\gamma T$  for  $k \geq 1$ , we obtain

$$g^{(1)}(t_{k-\frac{1}{2}}) = \frac{g_k - g_{k-1}}{\tau_k} + \frac{1}{24} \left( \frac{k}{N} \right)^{2\gamma} T^2 g^{(3)}(t_{k-\frac{1}{2}}) + \dots \quad (2.32)$$

□

Note that for  $n = 1, 2$ , we approximate first term of equation (2.33) using linear interpolation between points  $(t_0, v^0)$  and  $(t_{\frac{1}{2}}, v^{\frac{1}{2}})$ , and second term between  $(t_{\frac{1}{2}}, v^{\frac{1}{2}})$

and  $(t_{\frac{3}{2}}, v^{\frac{3}{2}})$ , respectively. Finally, we get

$$\begin{aligned} & {}^C\mathcal{D}_{0,t}^\alpha u(t_{\frac{3}{2}}) \\ &= \int_{t_0}^{t_{\frac{1}{2}}} \omega_{2-\alpha}(t_{\frac{1}{2}} - s) v'(s) ds + \int_{t_{\frac{1}{2}}}^{t_{\frac{3}{2}}} \omega_{2-\alpha}(t_{\frac{3}{2}} - s) v'(s) ds, \end{aligned} \quad (2.33)$$

$$\begin{aligned} &= \int_0^{t_{\frac{1}{2}}} \omega_{2-\alpha}(t_{\frac{1}{2}} - s) \left\{ \frac{v^{\frac{1}{2}} - v^0}{t_{\frac{1}{2}}} \right\} ds + r^1 + \int_{t_{\frac{1}{2}}}^{t_{\frac{3}{2}}} \omega_{2-\alpha}(t_{\frac{3}{2}} - s) \left\{ \frac{v^{\frac{3}{2}} - v^{\frac{1}{2}}}{t_{\frac{3}{2}} - t_{\frac{1}{2}}} \right\} ds, \\ &= \frac{1}{\Gamma(3-\alpha)} \left[ \left( \frac{\tau_1}{2} \right)^{1-\alpha} \left( \frac{v^1 - v^0}{2} \right) + \left( \frac{\tau_1 + \tau_2}{2} \right)^{1-\alpha} \left( \frac{v^2 - v^0}{2} \right) \right] + r^1 + r^2, \end{aligned} \quad (2.34)$$

where

$$r^1 = \int_0^{t_{\frac{1}{2}}} \omega_{2-\alpha}(t_{\frac{1}{2}} - s) \left\{ v'(s) - \frac{v^{\frac{1}{2}} - v^0}{t_{\frac{1}{2}} - t_0} \right\} ds \leq \hat{C}_1 \max_{t_0 \leq \hat{\eta}_1 \leq t_{\frac{1}{2}}} |v''(\hat{\eta}_1)| (\tau_1)^{3-\alpha}$$

and

$$r^2 = \int_{t_{\frac{1}{2}}}^{t_{\frac{3}{2}}} \omega_{2-\alpha}(t_{\frac{3}{2}} - s) \left\{ v'(s) - \frac{v^{\frac{3}{2}} - v^{\frac{1}{2}}}{t_{\frac{3}{2}} - t_{\frac{1}{2}}} \right\} ds \leq \hat{C}_2 \max_{t_{\frac{1}{2}} \leq \hat{\eta}_2 \leq t_{\frac{3}{2}}} |v''(\hat{\eta}_2)| (\tau_1 + \tau_2)^{3-\alpha}.$$

Combining equations (2.27) and (2.34), we obtain the approximation formula for the TFCD of order  $1 < \alpha < 2$  as

$${}^C\mathcal{D}_{0,t}^\alpha u(t_{\frac{1}{2}}) = \frac{(\tau_1)^{1-\alpha}}{2^{2-\alpha} \Gamma(3-\alpha)} (v^1 - v^0) + r^1, \quad (2.35)$$

$$v^{\frac{1}{2}} \approx \delta_t u^{\frac{1}{2}}, \quad (2.36)$$

$${}^C\mathcal{D}_{0,t}^\alpha u(t_{\frac{3}{2}}) = \frac{(\tau_1)^{1-\alpha}}{2^{2-\alpha} \Gamma(3-\alpha)} (v^1 - v^0) + \frac{(\tau_1 + \tau_2)^{1-\alpha}}{2^{2-\alpha} \Gamma(3-\alpha)} (v^2 - v^0) + r^2, \quad (2.37)$$

$$v^{\frac{3}{2}} \approx \delta_t u^{\frac{3}{2}}, \quad (2.38)$$

$${}^C\mathcal{D}_{0,t}^\alpha u(t_{n-\frac{1}{2}}) = d_0^{(n)} \left[ \frac{v^n + v^{n-1}}{2} \right] - \sum_{k=1}^{n-1} (d_{n-k-1}^{(n)} - d_{n-k}^{(n)}) \left[ \frac{v^k + v^{k-1}}{2} \right] - d_{n-1}^{(n)} v^0 + r^{n-\frac{1}{2}}, \quad (2.39)$$

$$v^{n-\frac{1}{2}} \approx \delta_t u^{n-\frac{1}{2}}, \quad n \geq 3. \quad (2.40)$$

**(R2)** For  $\alpha \in (1, 2)$ , and the regularity condition on  $u(t) \in C^3[0, T] \cap C^4(0, T]$ , the local truncation error bound for  $n \geq 3$  is obtained as:

$$\begin{aligned} |r^n| &= \left| \int_0^{t_1} \omega_{2-\alpha}(t_n - s) [v(s) - \Pi_{1,1}v(s)]' ds \right. \\ &\quad \left. + \sum_{k=2}^{n-1} \int_{t_{k-1}}^{t_k} \omega_{2-\alpha}(t_n - s) [v(s) - \Pi_{2,k}v(s)]' ds \right|, \\ &= \left| \frac{1}{2!} \int_0^{t_1} (s - t_0)(s - t_1)(t_n - s)^{-\alpha} v''(s) ds \right. \\ &\quad \left. + \frac{1}{3!} \sum_{k=2}^{n-1} \int_{t_{k-1}}^{t_k} (t_n - s)^{-\alpha} (s - t_{k-2})(s - t_{k-1})(s - t_k) v'''(s) ds \right. \\ &\quad \left. - \frac{1}{3!} \int_{t_{n-1}}^{t_n} (t_n - s)^{1-\alpha} (s - t_{n-2})(s - t_{n-1}) v'''(s) ds \right| := I + II + III, \quad (2.41) \end{aligned}$$

$$\begin{aligned} I &:= \left| \frac{1}{2!} \int_0^{t_1} (s - t_0)(s - t_1)(t_n - s)^{-\alpha} v''(s) ds \right| \\ &\leq C_1 \max_{t_0 \leq \eta_1 \leq t_1} |v''(\eta_1)| (t_n - t_1)^{-\alpha} \tau_1^3, \\ &\leq C_1 \max_{t_0 \leq \eta_1 \leq t_1} |v''(\eta_1)| (\tau_n + \tau_2)^{-\alpha} \tau_1^3, \\ &\leq C_1 \max_{t_0 \leq \eta_1 \leq t_1} |v''(\eta_1)| \frac{T^{3-\alpha}}{N^{(3-\alpha)\gamma}}. \quad (2.42) \end{aligned}$$

$$\begin{aligned} II &:= \left| \frac{1}{3!} \sum_{k=2}^{n-1} \int_{t_{k-1}}^{t_k} (t_n - s)^{-\alpha} (s - t_{k-2})(s - t_{k-1})(s - t_k) v'''(s) ds \right| \\ &\leq C_2 \max_{t_0 \leq \eta_2 \leq t_1} |v'''(\eta_2)| \sum_{k=2}^{n-1} \tau_k^3 (\tau_{k-1} + \tau_k) (t_n - t_k)^{-\alpha}, \\ &\leq C_2 \max_{t_0 \leq \eta_2 \leq t_1} |v'''(\eta_2)| \frac{T^{4-\alpha}}{N^{(4-\alpha)\gamma}}. \quad (2.43) \end{aligned}$$

$$\begin{aligned}
III &:= \left| \frac{1}{3!} \int_{t_{n-1}}^{t_n} (t_n - s)^{1-\alpha} (s - t_{n-2})(s - t_{n-1}) v'''(s) ds \right| \\
&\leq C_3 \max_{t_0 \leq \eta_3 \leq t_1} |v'''(\eta_3)| \frac{T^{4-\alpha}}{N^{(4-\alpha)\gamma}}, \tag{2.44}
\end{aligned}$$

where  $C_1, C_2, C_3$  are constants. Since,  $r^{n-\frac{1}{2}} = \frac{r^n + r^{n-1}}{2}$ , we get

$$|r^{n-\frac{1}{2}}| \leq C_1 \max_{t_0 \leq t \leq t_1} |u'''(t)| \frac{T^{3-\alpha}}{N^{(3-\alpha)\gamma}} + C_2 \max_{t_0 \leq \tilde{t} \leq t_n} |u''''(\tilde{t})| \frac{T^{4-\alpha}}{N^{(4-\alpha)\gamma}}, \quad n \geq 3. \tag{2.45}$$

*Lemma 2.2.3.* (i) For  $1 < \alpha < 2$ , the coefficients  $\{b_{n-k}^{(n)}, 1 \leq k \leq n\}$  defined in (2.24) hold:

$$0 < b_{n-k+1}^{(n)} < b_{n-k}^{(n)}, \quad 1 \leq k \leq n.$$

(ii) The coefficients  $c_{n-k}^{(n)}$ , ( $k \geq 2$ ) defined in (2.25) satisfy:

$$0 < c_{n-k}^{(n)} \leq \frac{1}{4\zeta_k(1 + \zeta_k)} \int_{t_{k-1}}^{t_k} \omega_{1-\alpha}(t_n - s) ds.$$

*Proof.* (i) For  $k = n$ , we have  $b_0^{(n)} = \frac{1}{(2-\alpha)} \omega_{2-\alpha}(t_n - t_{n-1}) > \omega_{2-\alpha}(t_n - t_{n-1})$ , and for  $1 \leq k < n$ , the inequalities hold from the mean value theorem as  $\omega_{2-\alpha}(t_n - s)$  is monotonic increasing.

(ii) From equation (2.26), and  $0 < (s - t_{k-1})(t_k - s) < \frac{\tau_k^2}{4}$ ,  $s \in (t_{k-1}, t_k)$ , we get the required result.  $\square$

*Lemma 2.2.4.* [126] The discrete coefficients  $d_{n-k}^{(n)}$ ,  $1 \leq k \leq n$  defined in (2.23) are monotonic and positive:

$$d_0^{(n)} \geq d_1^{(n)} \geq \dots \geq d_{n-1}^{(n)}, \quad 1 \leq k \leq n. \tag{2.46}$$

**Test example to verify approximation methods for TFCD:** Before using the approximation methods (2.7) and (2.35)-(2.40) to solve the TFDW equation, we first

check the numerical results for approximations of TFCD of a function  $u$ . If  $u$  is not satisfying the regularity conditions **R1** and **R2**, then we use nonuniform meshes to get the desired accuracy.

*Example 2.2.1.* Let  $u(t) = 1 + \omega_{1+\rho}(t)$ , then  ${}^C\mathcal{D}_{0,t}^\alpha u(t) = \frac{t^{\rho-\alpha}}{\Gamma(1+\rho-\alpha)}$ ,  $1 < \alpha < 2$ .

Now, we calculate the numerical results for  $\alpha$ -th order TFCD of  $u$  using nonuniform approximation methods (2.7) and (2.35)-(2.40).

TABLE 2.1: Maximum error and convergence order for the Example 2.2.1 with  $\rho = (2 + \alpha)$ .

$\tau$	$(\alpha, \gamma)$	Scheme (2.7)			Scheme (2.35)-(2.40)		
		$\ u^\tau - U^\tau\ _\infty$	OC	CPU(s)	$\ u^\tau - U^\tau\ _\infty$	OC	CPU(s)
$1/2^3$	(1.25, 1)	1.5709E-02		1.576561	1.1435E-03		3.871147
$1/2^4$		4.7288E-03	1.7320	4.548642	2.8587E-04	2.0000	10.61340
$1/2^5$		1.4188E-03	1.7368	9.967772	7.1468E-05	2.0000	25.08490
$1/2^6$		4.2501E-04	1.7391	20.92040	1.7867E-05	2.0000	53.34022
$1/2^7$		1.2720E-04	1.7404	46.18314	4.4668E-06	2.0000	106.5502
$1/2^8$		3.8043E-05	1.7414	98.35677	1.1167E-06	2.0000	237.3018
$1/2^3$	(1.5, 1)	3.3451E-02		1.617252	2.5073E-03		2.516321
$1/2^4$		1.2202E-02	1.4549	4.681029	6.2683E-04	2.0000	6.128888
$1/2^5$		4.3943E-03	1.4734	10.63620	1.5671E-04	2.0000	13.38468
$1/2^6$		1.5714E-03	1.4836	23.06959	3.9177E-05	2.0000	28.23417
$1/2^7$		5.5964E-04	1.4895	51.67087	9.7943E-06	2.0000	58.25899
$1/2^8$		1.9881E-04	1.4931	104.0464	2.4486E-06	2.0000	121.7009
$1/2^3$	(1.75, 1)	6.5242E-02		3.207947	3.9150E-03		2.767470
$1/2^4$		2.8457E-02	1.1970	8.971787	9.7876E-04	2.0000	8.031380
$1/2^5$		1.2192E-02	1.2228	21.18026	2.4469E-04	2.0000	24.85320
$1/2^6$		5.1774E-03	1.2357	47.44387	6.1172E-05	2.0000	45.92955
$1/2^7$		2.1884E-03	1.2423	92.64518	1.5293E-05	2.0000	109.2989
$1/2^8$		9.2275E-04	1.2459	184.5107	3.8233E-06	2.0000	221.2529

Figure 2.2 displays the absolute error for  $u(t) = t^{4+\alpha}$  using the approximation methods given in (2.7) and (2.35)-(2.40) for different values of  $\alpha = 1.2, 1.3, 1.4, 1.5, 1.6, 1.7, 1.8$  and  $T = 1$ . Figures (a) and (b) are the error plots corresponding to uniform discretization as  $\gamma = 1$  in approximation method (2.7) and (2.35)-(2.40). However,

Figures **(c)**, **(d)**, **(e)**, **(f)** show the error plot for nonuniform as  $\gamma > 1$ . From these figures we can note the effectiveness of the nonuniform meshes near the initial time  $t = 0$ . From Figures **(c)**, **(d)**, **(e)**, **(f)**, we observe that the error remains smaller for larger time intervals in comparison to Figures **(a)** and **(b)**.

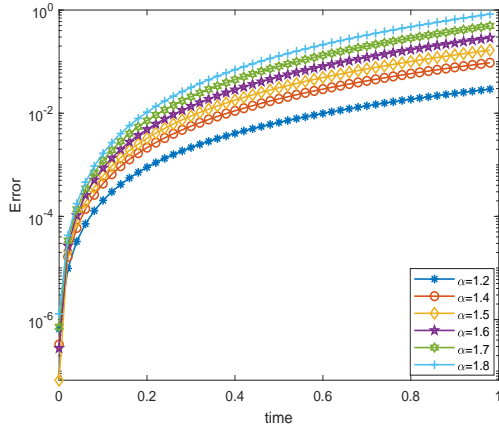
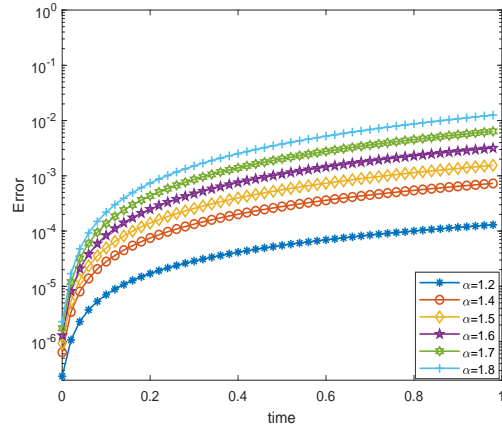
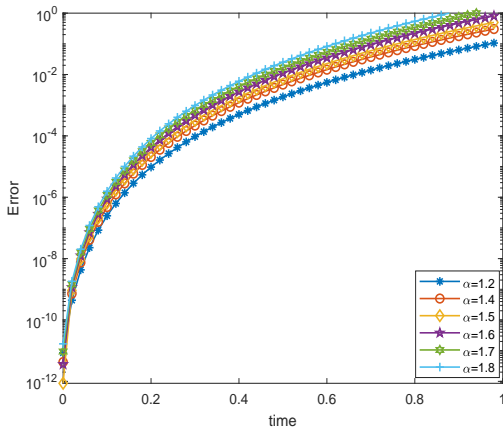
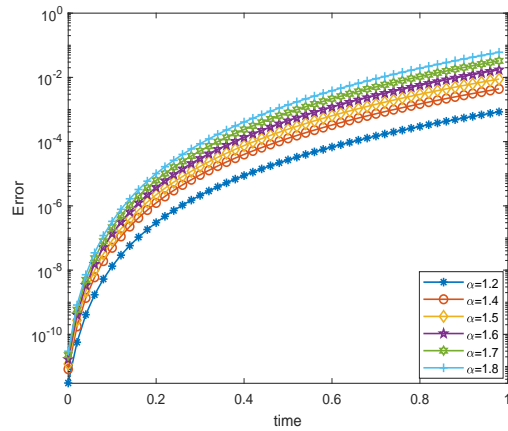
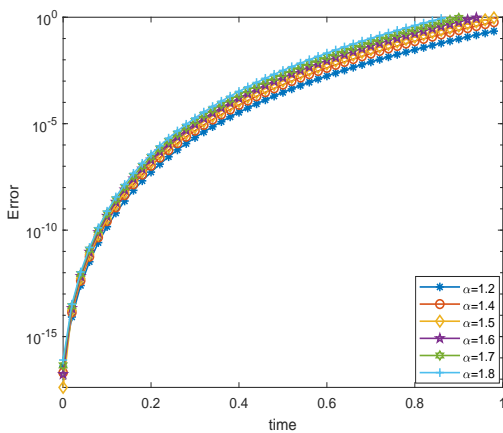
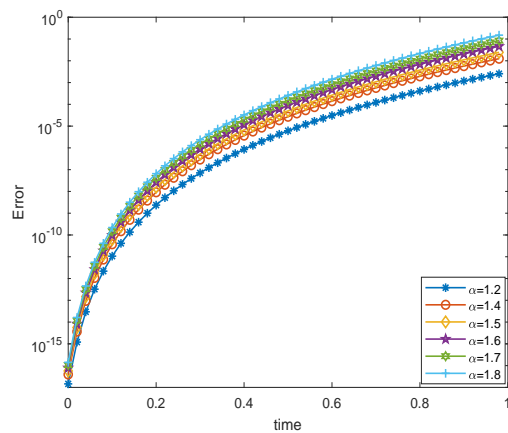
(a) For scheme (2.7) with  $\gamma = 1$ .(b) For scheme (2.35)-(2.40) with  $\gamma = 1$ .(c) For scheme (2.7) with  $\gamma = 2$ .(d) For scheme (2.35)-(2.40) with  $\gamma = 2$ .(e) For scheme (2.7) with  $\gamma = 3$ .(f) For scheme (2.35)-(2.40) with  $\gamma = 3$ .

FIGURE 2.2: Comparison of schemes (2.7) and (2.35)-(2.40) via absolute error of the function  $u(t) = t^{4+\alpha}$  using the uniform and nonuniform mesh for the different values of  $\alpha$  with  $N = 50$ .

TABLE 2.2: Maximum error and convergence order for the Example 2.2.1 with  $\rho = (1 + \alpha)$ .

$\tau$	$(\alpha, \gamma)$	Scheme (2.7)			Scheme (2.35)-(2.40)			
		$\ u^\tau - U^\tau\ _\infty$	OC	CPU	$\ u^\tau - U^\tau\ _\infty$	OC	CPU	
$1/2^3$	(1.255, 2)	4.3009E-02		13.35178	1.9330E-03		2.953083	
$1/2^4$		1.0752E-02	2.0000	46.28261	4.8326E-04	2.0000	8.499666	
$1/2^5$		2.6881E-03	2.0000	120.8176	1.2081E-04	2.0000	52.70156	
$1/2^6$		6.7202E-04	2.0000	282.6810	3.0204E-05	2.0000	146.9893	
$1/2^7$		1.6800E-04	2.0000	536.0180	7.5509E-06	2.0000	322.3102	
$1/2^8$		4.2001E-05	2.0000	1002.912	1.8877E-06	2.0000	687.6997	
$1/2^3$		(1.555, 2.5)	8.5092E-02		12.12018	4.7209E-03		3.228855
$1/2^4$			3.1322E-02	1.4418	36.52268	8.3455E-04	2.5000	9.325238
$1/2^5$	1.1573E-02		1.4364	85.09192	1.4753E-04	2.5000	63.33174	
$1/2^6$	4.2670E-03		1.4394	175.8528	2.6080E-05	2.5000	162.6707	
$1/2^7$	1.5629E-03		1.4490	358.6897	4.6103E-06	2.5000	387.2866	
$1/2^8$	5.6317E-04		1.4726	728.9154	8.1499E-07	2.5000	816.0251	
$1/2^3$	(1.755, 3)	2.1184E-01		12.56735	4.9448E-03		12.87423	
$1/2^4$		8.8678E-02	1.2563	37.06015	1.0359E-03	2.2551	39.65175	
$1/2^5$		3.7347E-02	1.2476	86.83922	2.1819E-04	2.2472	105.1414	
$1/2^6$		1.5750E-02	1.2456	179.6416	4.6085E-05	2.2432	232.6552	
$1/2^7$		6.6323E-03	1.2478	367.9144	9.7636E-06	2.2388	439.4022	
$1/2^8$		2.7792E-03	1.2548	745.0688	2.0914E-06	2.2229	876.6694	

## 2.3 The Derivation of the Nonuniform Difference Schemes for Two-Dimensional Case

For spatial direction approximation, let  $h_1 = \frac{L_1}{M_1}$  and  $h_2 = \frac{L_2}{M_2}$ , ( $M_1, M_2$  are positive integers) be spatial step lengths with  $x_i = ih_1$  and  $y_j = jh_2$  as grid points in  $x$  and  $y$  directions, respectively. The mesh domain is defined by  $\Omega_s = \{(ih_1, jh_2) \mid 1 \leq i \leq M_1 - 1, 1 \leq j \leq M_2 - 1\}$ , and  $\bar{\Omega}_s = \Omega_s \cup \partial\Omega_s$  be the space domain including boundaries. The functions at grids are denoted as  $v(x_i, y_j, t_n) = v_{i,j}^n$ ,  $u(x_i, y_j, t_n) = u_{i,j}^n$  and  $f(x_i, y_j, t_n) = f_{i,j}^n$  for  $0 \leq n \leq N$ ,  $(i, j) \in [0, M_1] \times [0, M_2]$ . We define the space of grid functions as  $\mathfrak{U} = \{u(x_i, y_j) = u_{i,j} \mid (i, j) \in [0, M_1] \times [0, M_2]\}$  and  $\bar{\mathfrak{U}} = \{u_{i,j} \in \mathfrak{U} \mid u_{i,j} = 0, (i, j) \in \partial\Omega_s\}$ .

In the grid space  $\mathfrak{U}$ , we denote the following operators:

$$\left\{ \begin{array}{l} \delta_x u_{i-\frac{1}{2},j}^n = \frac{u_{i,j}^n - u_{i-1,j}^n}{h_x}, \quad \delta_{xx} u_{i,j}^n = \frac{u_{i+1,j}^n - 2u_{i,j}^n + u_{i-1,j}^n}{h_x^2}, \\ \delta_y u_{i,j-\frac{1}{2}}^n = \frac{u_{i,j}^n - u_{i,j-1}^n}{h_y}, \quad \delta_{yy} u_{i,j}^n = \frac{u_{i,j+1}^n - 2u_{i,j}^n + u_{i,j-1}^n}{h_y^2}, \\ \delta_y \delta_x u_{i-\frac{1}{2},j-\frac{1}{2}} = \frac{1}{h_1} (\delta_y u_{i,j-\frac{1}{2}} - \delta_y u_{i-1,j-\frac{1}{2}}), \\ \delta_y \delta_{xx} u_{i,j} = \frac{1}{h_1} (\delta_y \delta_{xx} u_{i+\frac{1}{2},j} - \delta_y \delta_{xx} u_{i-\frac{1}{2},j}), \\ \Delta_h u_{i,j} = \delta_{xx} u_{i,j} + \delta_{yy} u_{i,j}. \end{array} \right. \quad (2.47)$$

### 2.3.1 Nonuniform $L1$ Difference Scheme

Taking equations (1.9)-(1.11) at the grid point  $(x_i, y_j, t_n)$  and then using the approximation of TFCD (2.7), we get

$${}^C \mathcal{D}_{0,t}^\alpha u(x_i, y_j, t_n) = \Delta_h u(x_i, y_j, t_n) + f(x_i, y_j, t_n) + \mathfrak{R}_t^n + \mathfrak{R}_x^n, \quad (x_i, y_j) \in \Omega_s, \quad n \geq 1.$$

$$\begin{aligned}
& a_1^{(n)} \left\{ \frac{u_{i,j}^n - u_{i,j}^{n-1}}{\tau_n} \right\} + \sum_{k=1}^{n-1} (a_{n-k+1}^{(n)} - a_{n-k}^{(n)}) \left\{ \frac{u_{i,j}^k - u_{i,j}^{k-1}}{\tau_k} \right\} \\
& + F(n) \left\{ \frac{u_{i,j}^n - u_{i,j}^{n-1}}{\tau_n} - \frac{u_{i,j}^{n-1} - u_{i,j}^{n-2}}{\tau_{n-1}} \right\} - a_n^{(n)} v_{i,j}^0 = \Delta_h u_{i,j}^n + f_{i,j}^n + \mathfrak{R}_t^n + \mathfrak{R}_x^n, \quad (2.48)
\end{aligned}$$

$$u_{i,j}^n = \Phi(x_i, y_j, t_n), \quad (x_i, y_j) \in \Omega_s, \quad t \in (0, T], \quad (2.49)$$

$$u_{i,j}^0 = \phi(x_i, y_j), \quad v_{i,j}^0 = \varphi(x_i, y_j), \quad (x_i, y_j) \in \bar{\Omega}_s, \quad (2.50)$$

where  $F(n) = \frac{2^{\alpha-1}}{\Gamma(3-\alpha)} \frac{\tau_n^{2-\alpha}}{(\tau_{n-1} + \tau_n)} > 0$ ,  $n \geq 2$ , and  $F(1) = \frac{2^{\alpha-1}}{\Gamma(3-\alpha)} \tau_1^{1-\alpha}$ .

Now, equation (2.48) can be rewritten as,

$$\begin{aligned}
& \frac{a_1^{(n)} + F(1)}{\tau_1} (u_{i,j}^1 - u_{i,j}^0) = (a_1^{(n)} + F(1)) v_{i,j}^0 + \Delta_h u_{i,j}^n \\
& \quad + f_{i,j}^n + (r_1)_t^n + (r_1)_x^n, \quad n = 1, \quad (2.51)
\end{aligned}$$

$$\begin{aligned}
& \frac{a_1^{(n)} + F(n)}{\tau_n} (u_{i,j}^n - u_{i,j}^{n-1}) + \sum_{k=1}^{n-1} \frac{(a_{n-k+1}^{(n)} - a_{n-k}^{(n)})}{\tau_k} (u_{i,j}^k - u_{i,j}^{k-1}) \\
& - \frac{F(n)}{\tau_{n-1}} (u_{i,j}^{n-1} - u_{i,j}^{n-2}) = a_n^{(n)} v_{i,j}^0 + \Delta_h u_{i,j}^n + f_{i,j}^n + (r_2)_t^n + (r_2)_x^n, \quad n \geq 2. \quad (2.52)
\end{aligned}$$

Suppose,  $\tilde{\mu}_n = \frac{\tau_n}{a_1^{(n)} + F(n)} > 0$ ,  $n \geq 1$ , then equations (2.51) and (2.52) become

$$\begin{aligned}
& u_{i,j}^n - u_{i,j}^{n-1} = \tilde{\mu}_n \Delta_h u_{i,j}^n + \tilde{\mu}_n \sum_{k=1}^{n-1} \frac{a_{n-k}^{(n)} - a_{n-k+1}^{(n)}}{\tau_k} (u_{i,j}^k - u_{i,j}^{k-1}) \\
& \quad + \frac{\tilde{\mu}_n F(n)}{\tau_{n-1}} (u_{i,j}^{n-1} - u_{i,j}^{n-2}) + \tilde{\mu}_n a_n^{(n)} \psi_{i,j} + \tilde{\mu}_n f_{i,j}^n + \mathfrak{R}, \quad (2.53)
\end{aligned}$$

where the truncation error  $|\mathfrak{R}| \leq \tilde{C}(N^{-\gamma(3-\alpha)} + h_1^2 + h_2^2)$  with the positive constant  $\tilde{C}$ .

Omitting the error term from equation (2.53) and replacing the analytical solution

$u_{i,j}^n$  by its numerical solution  $U_{i,j}^n$ , we obtain

$$\begin{aligned} U_{i,j}^n - \tilde{\mu}_n \Delta_h U_{i,j}^n &= U_{i,j}^{n-1} + \tilde{\mu}_n \sum_{k=1}^{n-1} \frac{(a_{n-k}^{(n)} - a_{n-k+1}^{(n)})}{\tau_k} (U_{i,j}^k - U_{i,j}^{k-1}) + \frac{\tilde{\mu}_n F(n)}{\tau_{n-1}} (U_{i,j}^{n-1} \\ &- U_{i,j}^{n-2}) + \tilde{\mu}_n a_n^{(n)} v_{i,j}^0 + \tilde{\mu}_n f_{i,j}^n, \quad (x_i, y_j) \in \Omega_s, \quad 1 \leq n \leq N. \end{aligned} \quad (2.54)$$

To construct ADI scheme, we add a small term  ${}^C \mathcal{D}_{0,t}^\alpha \tilde{\mu}_n^2 \delta_x^2 \delta_y^2 U_{i,j}^n$  to equation (2.54),

$$\begin{aligned} (I - \tilde{\mu}_n \delta_x^2)(I - \tilde{\mu}_n \delta_y^2) U_{i,j}^n &= (U_{i,j}^{n-1} + \tilde{\mu}_n^2 \delta_x^2 \delta_y^2 U_{i,j}^{n-1}) + \tilde{\mu}_n \sum_{k=1}^{n-1} \frac{(a_{n-k}^{(n)} - a_{n-k+1}^{(n)})}{\tau_k} \\ &(U_{i,j}^k + \tilde{\mu}_n^2 \delta_x^2 \delta_y^2 U_{i,j}^k - U_{i,j}^{k-1} - \tilde{\mu}_n^2 \delta_x^2 \delta_y^2 U_{i,j}^{k-1}) + \frac{\tilde{\mu}_n F(n)}{\tau_{n-1}} (U_{i,j}^{n-1} + \tilde{\mu}_n^2 \delta_x^2 \delta_y^2 U_{i,j}^{n-1} \\ &- U_{i,j}^{n-2} - \tilde{\mu}_n^2 \delta_x^2 \delta_y^2 U_{i,j}^{n-2}) + \tilde{\mu}_n a_n^{(n)} v_{i,j}^0 + \tilde{\mu}_n f_{i,j}^n, \quad n \geq 1. \end{aligned} \quad (2.55)$$

Suppose  $W_{i,j}^*$  is the intermediate variable define as  $W_{i,j}^* = (I - \tilde{\mu}_n \delta_y^2) U_{i,j}^n$ ,  $0 \leq i \leq M_1$ ,  $1 \leq j \leq M_2 - 1$ .

Firstly, we solve the following system of equations to find the intermediate variable  $W_{i,j}^*$ , for fixed  $j \in \{1, 2, \dots, M_2 - 1\}$ ,

$$\begin{aligned} (I - \tilde{\mu}_n \delta_x^2) W_{i,j}^* &= (U_{i,j}^{n-1} + \tilde{\mu}_n^2 \delta_x^2 \delta_y^2 U_{i,j}^{n-1}) + \tilde{\mu}_n \sum_{k=1}^{n-1} \frac{(a_{n-k}^{(n)} - a_{n-k+1}^{(n)})}{\tau_k} (U_{i,j}^k \\ &+ \tilde{\mu}_n^2 \delta_x^2 \delta_y^2 U_{i,j}^k - U_{i,j}^{k-1} - \tilde{\mu}_n^2 \delta_x^2 \delta_y^2 U_{i,j}^{k-1}) + \frac{\tilde{\mu}_n F(n)}{\tau_{n-1}} (U_{i,j}^{n-1} + \tilde{\mu}_n^2 \delta_x^2 \delta_y^2 U_{i,j}^{n-1} \\ &- U_{i,j}^{n-2} - \tilde{\mu}_n^2 \delta_x^2 \delta_y^2 U_{i,j}^{n-2}) - \tilde{\mu}_n a_n v_{i,j}^0 + \tilde{\mu}_n f_{i,j}^n, \quad 1 \leq i \leq M_1 - 1, \end{aligned} \quad (2.56)$$

$$W_{0,j}^* = (I - \tilde{\mu}_n \delta_y^2) U_{0,j}^n, \quad W_{M_1,j}^* = (I - \tilde{\mu}_n \delta_y^2) U_{M_1,j}^n, \quad (2.57)$$

when  $W_{i,j}^*$  is available, then we solve the following system of equations to get final numerical solution  $U_{i,j}^n$ , for fixed  $i \in \{1, 2, \dots, M_1 - 1\}$

$$(I - \tilde{\mu}_n \delta_y^2) U_{i,j}^n = W_{i,j}^*, \quad 1 \leq j \leq M_2 - 1, \quad (2.58)$$

$$U_{i,0}^n = \Phi(x_i, 0, t_n), \quad U_{i,M_2}^n = \Phi(x_i, L_2, t_n). \quad (2.59)$$

### 2.3.2 Nonuniform Crank-Nicolson $L1 - 2$ Difference Scheme

Before introducing the difference scheme to find the solution  $u$  of the problem (1.9)-(1.11), we define some regularity conditions on  $u$ .

**(R3)**  $u \in C_{(x,y,t)}^{(0,0,3)}(\bar{\Omega} \times [0, T]) \cap C_{(x,y,t)}^{(0,0,4)}(\bar{\Omega} \times (0, T])$ , then  $|\partial_t^{(4)}u(x, y, t)| \leq \bar{C}t^{\alpha-2}$ ,  $(x, y) \in \bar{\Omega}$ ,  $0 < t \leq T$ , where  $\bar{C}$  is a positive constant. Then we obtain from the approximation of Caputo derivative equations (2.35), (2.37), (2.39)

$$\left\{ \begin{array}{l} C\mathcal{D}_{0,t}^\alpha u_{i,j}^{\frac{1}{2}} = \frac{\tau_1^{1-\alpha}}{2^{2-\alpha}\Gamma(3-\alpha)}(v_{i,j}^1 - v_{i,j}^0) + r^1, \quad (x_i, y_j) \in \Omega_s, \quad n = 1, \\ C\mathcal{D}_{0,t}^\alpha u_{i,j}^{\frac{3}{2}} = \frac{\tau_1^{1-\alpha}}{2^{2-\alpha}\Gamma(3-\alpha)}(v_{i,j}^1 - v_{i,j}^0) \\ \quad + \frac{(\tau_1+\tau_2)^{1-\alpha}}{2^{2-\alpha}\Gamma(3-\alpha)}(v_{i,j}^2 - v_{i,j}^0) + r^2, \quad (x_i, y_j) \in \Omega_s, \quad n = 2, \\ C\mathcal{D}_{0,t}^\alpha u_{i,j}^{n-\frac{1}{2}} = d_0^{(n)} \left[ \frac{v_{i,j}^n + v_{i,j}^{n-1}}{2} \right] - \sum_{k=1}^{n-1} (d_{n-k-1}^{(n)} \\ \quad - d_{n-k}^{(n)}) \left[ \frac{v_{i,j}^k + v_{i,j}^{k-1}}{2} \right] - d_{n-1}^{(n)} v_{i,j}^0 + r^{n-\frac{1}{2}}, \quad n \geq 3, \\ v_{i,j}^{n-\frac{1}{2}} = \delta_t u_{i,j}^{n-\frac{1}{2}} + r_{i,j}^n, \quad (x_i, y_j) \in \Omega_s, \quad n \geq 1, \\ |(R^{\frac{1}{2}})_{i,j}| \leq c_1(\tau_n)^{3-\alpha}, \quad |(R^{n-\frac{1}{2}})_{i,j}| \leq c_2(\tau_n)^{4-\alpha}, \quad n \geq 1. \end{array} \right. \quad (2.60)$$

**(R4)** Let  $\delta_x^2 u \in C_{(x,y,t)}^{(0,0,2)}(\bar{\Omega} \times [0, T])$  and  $\delta_y^2 u \in C_{(x,y,t)}^{(0,0,2)}(\bar{\Omega} \times [0, T])$ , and  $v = u'$ , then we obtains

$$\left\{ \begin{array}{l} \delta_t(\Delta_h u_{i,j}^{n-\frac{1}{2}}) = \Delta_h v_{i,j}^{n-\frac{1}{2}} + \mathcal{O}(T^2), \quad (x_i, y_j) \in \Omega_s, \quad n \geq 1, \\ \Delta_h u_{i,j}^n = \Delta_h u_{i,j}^{n-1} + \frac{\tau_n}{2}(\Delta_h v_{i,j}^n + \Delta_h v_{i,j}^{n-1}) + \mathcal{O}(\tau_n^2), \quad (x_i, y_j) \in \Omega_s, \quad n \geq 1. \end{array} \right. \quad (2.61)$$

Suppose  $u(x, y, t) \in C^{(4,4,4)}(\overline{\Omega} \times (0, T])$ , and then equations (1.9)-(1.11) at the grid point  $(x_i, y_j, t_{n-\frac{1}{2}})$

$${}^C\mathcal{D}_{0,t}^\alpha u_{i,j}^{n-\frac{1}{2}} = \Delta_h u_{i,j}^{n-\frac{1}{2}} + f_{i,j}^{n-\frac{1}{2}} + \mathfrak{R}_1^{n-\frac{1}{2}}, \quad (x_i, y_j) \in \Omega_s, \quad 1 \leq n \leq N, \quad (2.62)$$

$$u_{i,j}^n = \Phi(x_i, y_j, t_n), \quad (x_i, y_j) \in \Omega_s, \quad t \in (0, T], \quad (2.63)$$

$$u_{i,j}^0 = \phi(x_i, y_j), \quad v_{i,j}^0 = \varphi(x_i, y_j), \quad (x_i, y_j) \in \overline{\Omega}_s. \quad (2.64)$$

Using equations (2.60) and (2.61) into equation (2.62). Then, we have

$$\begin{aligned} v_{i,j}^1 &= v_{i,j}^0 + \frac{4}{\tau_1} \mu_1 \Delta_h u_{i,j}^0 + \mu_1 (\Delta_h v_{i,j}^1 + \Delta_h v_{i,j}^0) \\ &\quad + \frac{4}{\tau_1} \mu_1 f_{i,j}^{\frac{1}{2}} + \mathfrak{R}_1^{\frac{1}{2}}, \quad (x_i, y_j) \in \Omega_s, \quad n = 1, \end{aligned} \quad (2.65)$$

$$\begin{aligned} v_{i,j}^2 &= v_{i,j}^0 - \left(1 + \frac{\tau_2}{\tau_1}\right)^{\alpha-1} (v_{i,j}^1 - v_{i,j}^0) + \frac{4}{\tau_2} \mu_2 \Delta_h u_{i,j}^1 + \mu_2 (\Delta_h v_{i,j}^2 + \Delta_h v_{i,j}^1) \\ &\quad + \frac{4}{\tau_2} \mu_2 f_{i,j}^{\frac{3}{2}} + \mathfrak{R}_2^{\frac{3}{2}}, \quad (x_i, y_j) \in \Omega_s, \quad n = 2, \end{aligned} \quad (2.66)$$

$$\begin{aligned} v_{i,j}^n &= \frac{4}{\tau_n} \mu_3 d_{n-1}^{(n)} v_{i,j}^0 - v_{i,j}^{n-1} + \sum_{k=1}^{n-1} \frac{d_{n-k-1}^{(n)} - d_{n-k}^{(n)}}{d_0^{(n)}} (v_{i,j}^k + v_{i,j}^{k-1}) + \frac{4}{\tau_n} \mu_3 \Delta_h u_{i,j}^{n-1} \\ &\quad + \mu_3 (\Delta_h v_{i,j}^n + \Delta_h v_{i,j}^{n-1}) + \frac{4}{\tau_n} \mu_3 f_{i,j}^{n-\frac{1}{2}} + \mathfrak{R}^{n-\frac{1}{2}}, \quad (x_i, y_j) \in \Omega_s, \quad n \geq 3. \end{aligned} \quad (2.67)$$

Where  $\mu_1 = \frac{\Gamma(3-\alpha)}{2^\alpha} \tau_1^\alpha$ ,  $\mu_2 = \frac{\Gamma(3-\alpha)}{2^\alpha} \frac{\tau_2}{(\tau_1 + \tau_2)^{1-\alpha}}$  and  $\mu_3 = \frac{\tau_n}{2d_0^{(n)}}$ . To construct ADI scheme, we add a small term  ${}^C\mathcal{D}_{0,t}^\alpha \mu_1^2 \delta_x^2 \delta_y^2 u_{i,j}^{\frac{1}{2}}$ ,  ${}^C\mathcal{D}_{0,t}^\alpha \mu_2^2 \delta_x^2 \delta_y^2 u_{i,j}^{\frac{3}{2}}$  and  ${}^C\mathcal{D}_{0,t}^\alpha \mu_3^2 \delta_x^2 \delta_y^2 u_{i,j}^{n-\frac{1}{2}}$  into equations (2.65), (2.66), (2.67), respectively. Then we obtain

$$\begin{aligned} (I - \mu_1 \delta_x^2)(I - \mu_1 \delta_y^2) v_{i,j}^1 &= (v_{i,j}^0 + \mu_1^2 \delta_x^2 \delta_y^2 v_{i,j}^0) + \frac{4}{\tau_1} \mu_1 \Delta_h u_{i,j}^0 + \mu_1 \Delta_h v_{i,j}^0 + \frac{4}{\tau_1} \mu_1 f_{i,j}^{\frac{1}{2}} \\ &\quad + \mathfrak{R}_{i,j}^{\frac{1}{2}}, \quad (x_i, y_j) \in \Omega_s, \quad n = 1, \end{aligned} \quad (2.68)$$

$$\begin{aligned} (I - \mu_2 \delta_x^2)(I - \mu_2 \delta_y^2) v_{i,j}^2 &= (v_{i,j}^0 + \mu_2^2 \delta_x^2 \delta_y^2 v_{i,j}^0) - \left(1 + \frac{\tau_2}{\tau_1}\right)^{\alpha-1} (v_{i,j}^1 + \mu_2^2 \delta_x^2 \delta_y^2 v_{i,j}^1 - v_{i,j}^0 \\ &\quad - \mu_2^2 \delta_x^2 \delta_y^2 v_{i,j}^0) + \frac{4}{\tau_2} \mu_2 \Delta_h u_{i,j}^1 + \mu_2 \Delta_h v_{i,j}^1 + \frac{4}{\tau_2} \mu_2 f_{i,j}^{\frac{3}{2}} + \mathfrak{R}_{i,j}^{\frac{3}{2}}, \quad (x_i, y_j) \in \Omega_s, \quad n = 2, \end{aligned} \quad (2.69)$$

$$\begin{aligned}
(I - \mu_3 \delta_x^2)(I - \mu_3 \delta_y^2)v_{i,j}^n &= \frac{4}{\tau_n} \mu_3 d_{n-1}^{(n)} (v_{i,j}^0 + \mu_3^2 \delta_x^2 \delta_y^2 v_{i,j}^0) - (v_{i,j}^{n-1} + \mu_3^2 \delta_x^2 \delta_y^2 v_{i,j}^{n-1}) \\
&+ \sum_{k=1}^{n-1} \frac{d_{n-k-1}^{(n)} - d_{n-k}^{(n)}}{d_0^{(n)}} (v_{i,j}^k + \mu_3^2 \delta_x^2 \delta_y^2 v_{i,j}^k + v_{i,j}^{k-1} + \mu_3^2 \delta_x^2 \delta_y^2 v_{i,j}^{k-1}) + \frac{4}{\tau_n} \mu_3 \Delta_h u_{i,j}^{n-1} \\
&+ \mu_3 \Delta_h v_{i,j}^{n-1} + \frac{4}{\tau_n} \mu_3 f_{i,j}^{n-\frac{1}{2}} + \mathfrak{R}^{n-\frac{1}{2}}_{i,j}, \quad (x_i, y_j) \in \Omega_s, \quad n \geq 3. \tag{2.70}
\end{aligned}$$

Omitting the error term from the equations (2.68), (2.69), (2.70) and replacing exact solution  $u_{i,j}^n$  by the approximate solution  $U_{i,j}^n$  and also corresponding  $v_{i,j}^n$  by  $V_{i,j}^n$ , we have

$$\begin{aligned}
(I - \mu_1 \delta_x^2)(I - \mu_1 \delta_y^2)V_{i,j}^1 &= (v_{i,j}^0 + \mu_1^2 \delta_x^2 \delta_y^2 v_{i,j}^0) + \frac{4}{\tau_1} \mu_1 \Delta_h u_{i,j}^0 \\
&+ \mu_1 \Delta_h v_{i,j}^0 + \frac{4}{\tau_1} \mu_1 f_{i,j}^{\frac{1}{2}}, \quad (x_i, y_j) \in \Omega_s, \quad n = 1, \tag{2.71}
\end{aligned}$$

$$\begin{aligned}
(I - \mu_2 \delta_x^2)(I - \mu_2 \delta_y^2)V_{i,j}^2 &= (v_{i,j}^0 + \mu_2^2 \delta_x^2 \delta_y^2 v_{i,j}^0) - \left(1 + \frac{\tau_2}{\tau_1}\right)^{\alpha-1} (V_{i,j}^1 \\
&+ \mu_2^2 \delta_x^2 \delta_y^2 V_{i,j}^1 - v_{i,j}^0 - \mu_2^2 \delta_x^2 \delta_y^2 v_{i,j}^0) + \frac{4}{\tau_2} \mu_2 \Delta_h u_{i,j}^1 \\
&+ \mu_2 \Delta_h V_{i,j}^1 + \frac{4}{\tau_2} \mu_2 f_{i,j}^{\frac{3}{2}}, \quad (x_i, y_j) \in \Omega_s, \quad n = 2, \tag{2.72}
\end{aligned}$$

$$\begin{aligned}
(I - \mu_3 \delta_x^2)(I - \mu_3 \delta_y^2)V_{i,j}^n &= \frac{4}{\tau_n} \mu_3 d_{n-1}^{(n)} (v_{i,j}^0 + \mu_3^2 \delta_x^2 \delta_y^2 v_{i,j}^0) - (V_{i,j}^{n-1} + \mu_3^2 \delta_x^2 \delta_y^2 V_{i,j}^{n-1}) \\
&+ \sum_{k=1}^{n-1} \frac{d_{n-k-1}^{(n)} - d_{n-k}^{(n)}}{d_0^{(n)}} (V_{i,j}^k + \mu_3^2 \delta_x^2 \delta_y^2 V_{i,j}^k + V_{i,j}^{k-1} + \mu_3^2 \delta_x^2 \delta_y^2 V_{i,j}^{k-1}) \\
&+ \frac{4}{\tau_n} \mu_3 \Delta_h U_{i,j}^{n-1} + \mu_3 \Delta_h V_{i,j}^{n-1} + \frac{4}{\tau_n} \mu_3 f_{i,j}^{n-\frac{1}{2}}, \quad (x_i, y_j) \in \Omega_s, \quad n \geq 3. \tag{2.73}
\end{aligned}$$

Let  $W_{i,j}^* = (I - \mu_l \delta_y^2)V_{i,j}^l$ , ( $l = 1, 2, 3$ ) be the intermediate solution, for  $0 \leq i \leq M_1$ ,  $1 \leq j \leq M_2 - 1$ . Firstly, we solve the following system of equations for the intermediate solution  $W_{i,j}^*$ , for  $j \in \{1, 2, \dots, M_2 - 1\}$ ,

$$\begin{aligned}
(I - \mu_1 \delta_x^2)W_{i,j}^* &= (v_{i,j}^0 + \mu_1^2 \delta_x^2 \delta_y^2 v_{i,j}^0) + \frac{4}{\tau_1} \mu_1 \Delta_h u_{i,j}^0 + \mu_1 \Delta_h v_{i,j}^0 + \frac{4}{\tau_1} \mu_1 f_{i,j}^{\frac{1}{2}}, \\
&(x_i, y_j) \in \Omega_s, \quad n = 1, \tag{2.74}
\end{aligned}$$

$$(I - \mu_2 \delta_x^2)W_{i,j}^* = (v_{i,j}^0 + \mu_2^2 \delta_x^2 \delta_y^2 v_{i,j}^0) - \left(1 + \frac{\tau_2}{\tau_1}\right)^{\alpha-1} (V_{i,j}^1 + \mu_2^2 \delta_x^2 \delta_y^2 V_{i,j}^1 - v_{i,j}^0 - \mu_2^2 \delta_x^2 \delta_y^2 v_{i,j}^0) + \frac{4}{\tau_2} \mu_2 \Delta_h u_{i,j}^1 + \mu_2 \Delta_h V_{i,j}^1 + \frac{4}{\tau_2} \mu_2 f_{i,j}^{\frac{3}{2}}, \quad (x_i, y_j) \in \Omega_s, \quad n = 2, \quad (2.75)$$

$$(I - \mu_3 \delta_x^2)W_{i,j}^* = \frac{4}{\tau_n} \mu_3 d_{n-1}^{(n)} (v_{i,j}^0 + \mu_3^2 \delta_x^2 \delta_y^2 v_{i,j}^0) - (V_{i,j}^{n-1} + \mu_3^2 \delta_x^2 \delta_y^2 V_{i,j}^{n-1}) + \sum_{k=1}^{n-1} \frac{d_{n-k-1}^{(n)} - d_{n-k}^{(n)}}{d_0^{(n)}} (V_{i,j}^k + \mu_3^2 \delta_x^2 \delta_y^2 V_{i,j}^k + V_{i,j}^{k-1} + \mu_3^2 \delta_x^2 \delta_y^2 V_{i,j}^{k-1}) + \frac{4}{\tau_n} \mu_3 \Delta_h U_{i,j}^{n-1} + \mu_3 \Delta_h V_{i,j}^{n-1} + \frac{4}{\tau_n} \mu_3 f_{i,j}^{n-\frac{1}{2}}, \quad (x_i, y_j) \in \Omega_s, \quad n \geq 3, \quad (2.76)$$

$$W_{0,j}^* = (I - \mu_l \delta_y^2)V_{0,j}^n, \quad W_{M_1,j}^* = (I - \mu_l \delta_y^2)V_{M_1,j}^n, \quad l = 1, 2, 3. \quad (2.77)$$

For fixed  $i \in \{1, 2, \dots, M_1 - 1\}$ , we solve the following system

$$(I - \mu_l \delta_y^2)V_{i,j}^n = W_{i,j}^*, \quad 1 \leq j \leq M_2 - 1, \quad (2.78)$$

$$V_{i,0}^n = V(x_i, 0, t_n), \quad V_{i,M_2}^n = V(x_i, y_R, t_n), \quad (2.79)$$

we obtain the another intermediate solution  $V_{i,j}^n$ . To obtain final solution  $U_{i,j}^n$  using Lemma 2.2.2, we obtain

$$U_{i,j}^n = U_{i,j}^{n-1} + \frac{\tau_n}{2} (V_{i,j}^n + V_{i,j}^{n-1}), \quad n \geq 1, \quad (i, j) \in \Omega_s. \quad (2.80)$$

## 2.4 Stability Analysis

Here, we discuss the stability of both the difference schemes Nonuniform  $L1$  and Nonuniform Crank-Nicolson  $L1 - 2$  for the TFDW equation (1.9)-(1.11) in detail.

### 2.4.1 Stability Analysis for the Nonuniform $L1$ Difference Scheme

Suppose  $u_{i,j}^n$  and  $U_{i,j}^n$  are exact and approximate solutions of the equation (1.9)-(1.11) and Nonuniform  $L1$  difference scheme (2.55), respectively and denote

$$\mathcal{L}_{i,j}^n = U_{i,j}^n - u_{i,j}^n, \quad 1 \leq i \leq M_1 - 1, \quad 1 \leq j \leq M_2 - 1 \quad n = 1, 2, \dots, N. \quad (2.81)$$

We get the following roundoff error by using the equation (2.81) in difference scheme (2.55)

$$\begin{aligned} (I - \tilde{\mu}_n \delta_x^2)(I - \tilde{\mu}_n \delta_y^2) \mathcal{L}_{i,j}^n &= (\mathcal{L}_{i,j}^{n-1} + \tilde{\mu}_n^2 \delta_x^2 \delta_y^2 \mathcal{L}_{i,j}^{n-1}) \\ &+ \tilde{\mu}_n \sum_{k=1}^{n-1} \frac{(a_{n-k} - a_{n-k+1})}{\tau_k} (\mathcal{L}_{i,j}^k + \tilde{\mu}_n^2 \delta_x^2 \delta_y^2 \mathcal{L}_{i,j}^k - \mathcal{L}_{i,j}^{k-1} - \tilde{\mu}_n^2 \delta_x^2 \delta_y^2 \mathcal{L}_{i,j}^{k-1}) \\ &+ \frac{\tilde{\mu}_n F(n)}{\tau_{n-1}} (\mathcal{L}_{i,j}^{n-1} + \tilde{\mu}_n^2 \delta_x^2 \delta_y^2 \mathcal{L}_{i,j}^{n-1} - \mathcal{L}_{i,j}^{n-2} - \tilde{\mu}_n^2 \delta_x^2 \delta_y^2 \mathcal{L}_{i,j}^{n-2}) + \tilde{\mu}_n a_n \mathcal{L}_{i,j}^0. \end{aligned} \quad (2.82)$$

Now, we construct the grid function  $\mathcal{L}^n(x, y)$  as follows, for  $n = 1, 2, \dots, N$

$$\mathcal{L}^n(x, y) = \begin{cases} \mathcal{L}_{i,j}^n, & x_{i-\frac{1}{2}} < x \leq x_{i+\frac{1}{2}}, \quad y_{j-\frac{1}{2}} < y \leq y_{j+\frac{1}{2}} \\ & 1 \leq i \leq M_1 - 1, \quad 1 \leq j \leq M_2 - 1, \\ 0, & 0 \leq x \leq \frac{h_1}{2}, \quad l_1 - \frac{h_1}{2} < x \leq l_1, \\ & 0 \leq y \leq \frac{h_2}{2}, \quad l_2 - \frac{h_2}{2} < y \leq l_2. \end{cases} \quad (2.83)$$

The expression of the function  $\mathcal{L}^n(x, y)$  in Fourier series form is given as

$$\mathcal{L}^n(x, y) = \sum_{n_1=-\infty}^{\infty} \sum_{n_2=-\infty}^{\infty} \zeta^n(n_1, n_2) e^{2\pi i(n_1 x/l_1 + n_2 y/l_2)}, \quad n \geq 1, \quad (2.84)$$

where

$$\zeta^n(n_1, n_2) = \frac{1}{l_1 l_2} \int_0^{l_1} \int_0^{l_2} \mathcal{L}^n(x, y) e^{-2\pi i(n_1 x/l_1 + n_2 y/l_2)} dx dy. \quad (2.85)$$

Suppose the solution of equation (2.82) has the form  $\mathcal{L}_{i,j}^n = \zeta^n e^{\iota(i\tilde{\eta}_1 h_1 + j\tilde{\eta}_2 h_2)}$ , where,  $\tilde{\eta}_1 = 2\pi n_1/l_1$ ,  $\tilde{\eta}_2 = 2\pi n_2/l_2$ , and  $\iota = \sqrt{-1}$ . It can be easily obtained as

$$\delta_x^2 \mathcal{L}_{i,j}^n = -\frac{4}{h_1^2} \sin^2\left(\frac{\tilde{\eta}_1 h_1}{2}\right) \zeta^n e^{\iota(i\tilde{\eta}_1 h_1 + j\tilde{\eta}_2 h_2)}, \quad (2.86)$$

$$\delta_y^2 \mathcal{L}_{i,j}^n = -\frac{4}{h_2^2} \sin^2\left(\frac{\tilde{\eta}_2 h_2}{2}\right) \zeta^n e^{\iota(i\tilde{\eta}_1 h_1 + j\tilde{\eta}_2 h_2)}, \quad (2.87)$$

$$\delta_x^2 \delta_y^2 \mathcal{L}_{i,j}^n = \frac{16}{h_1^2 h_2^2} \sin^2\left(\frac{\tilde{\eta}_1 h_1}{2}\right) \sin^2\left(\frac{\tilde{\eta}_2 h_2}{2}\right) \zeta^n e^{\iota(i\tilde{\eta}_1 h_1 + j\tilde{\eta}_2 h_2)}. \quad (2.88)$$

Using the defined solution  $\mathcal{L}_{i,j}^n$  and expressions (2.86)-(2.88) into equation (2.82), we get

$$\begin{aligned} & \left[1 + \frac{4\tilde{\mu}_n}{h_1^2} \sin^2\left(\frac{\tilde{\eta}_1 h_1}{2}\right)\right] \left[1 + \frac{4\tilde{\mu}_n}{h_2^2} \sin^2\left(\frac{\tilde{\eta}_2 h_2}{2}\right)\right] \zeta^n = \left[1 + \frac{16\tilde{\mu}_n^2}{h_1^2 h_2^2} \sin^2\left(\frac{\tilde{\eta}_1 h_1}{2}\right) \right. \\ & \left. \sin^2\left(\frac{\tilde{\eta}_2 h_2}{2}\right)\right] \zeta^{n-1} + \tilde{\mu}_n \left[1 + \frac{16\tilde{\mu}_n^2}{h_1^2 h_2^2} \sin^2\left(\frac{\tilde{\eta}_1 h_1}{2}\right) \sin^2\left(\frac{\tilde{\eta}_2 h_2}{2}\right)\right] \\ & \left[\sum_{k=1}^{n-1} \frac{(a_{n-k}^{(n)} - a_{n-k+1}^{(n)})}{\tau_k} (\zeta^k - \zeta^{k-1}) + a_n \zeta^0\right] + \frac{\tilde{\mu}_n F(n)}{\tau_{n-1}} \left[\zeta^{n-1} - \zeta^{n-2} + \frac{16\tilde{\mu}_n^2}{h_1^2 h_2^2} \right. \\ & \left. \zeta^{n-1} \sin^2\left(\frac{\tilde{\eta}_1 h_1}{2}\right) \sin^2\left(\frac{\tilde{\eta}_2 h_2}{2}\right) - \frac{16\tilde{\mu}_n^2}{h_1^2 h_2^2} \zeta^{n-2} \sin^2\left(\frac{\tilde{\eta}_1 h_1}{2}\right) \sin^2\left(\frac{\tilde{\eta}_2 h_2}{2}\right)\right]. \quad (2.89) \end{aligned}$$

Let,

$$A = \frac{4\tilde{\mu}_n}{h_1^2} \sin^2\left(\frac{\tilde{\eta}_1 h_1}{2}\right) \geq 0, \quad B = \frac{4\tilde{\mu}_n}{h_2^2} \sin^2\left(\frac{\tilde{\eta}_2 h_2}{2}\right) \geq 0,$$

then, from equation (2.89) we get

$$\zeta^n = \frac{(1 + AB + \Xi_n) \zeta^{n-1} + \tilde{\mu}_n (1 + AB) \left[\sum_{k=1}^{n-1} \frac{(a_{n-k}^{(n)} - a_{n-k+1}^{(n)})}{\tau_k} (\zeta^k - \zeta^{k-1}) + a_n^{(n)} \zeta^0\right]}{(1 + A)(1 + B)}, \quad (2.90)$$

where  $\Xi_n = \frac{\tilde{\mu}_n F(n)}{\tau_{n-1}} - \frac{\tilde{\mu}_{n-1} F(n-1)}{\tau_{n-2}} \leq 0$ ,  $n > 2$ . Thus, we have

$$\zeta^n \leq \frac{(1 + AB)\zeta^{n-1} + \tilde{\mu}_n(1 + AB) \left[ \sum_{k=1}^{n-1} \frac{(a_{n-k}^{(n)} - a_{n-k+1}^{(n)})}{\tau_k} (\zeta^k - \zeta^{k-1}) + a_n^{(n)} \zeta^0 \right]}{(1 + A)(1 + B)}. \quad (2.91)$$

*Lemma 2.4.1.* For small value of  $h_1$  and  $h_2$ , the following inequality holds

$$\frac{\left| \left[ 1 + \frac{16\tilde{\mu}_n^2}{h_1^2 h_2^2} \sin^2 \left( \frac{\tilde{\eta}_1 h_1}{2} \right) \sin^2 \left( \frac{\tilde{\eta}_2 h_2}{2} \right) \right] \right|}{\left| \left[ 1 + \frac{4\tilde{\mu}_n}{h_1^2} \sin^2 \left( \frac{\tilde{\eta}_1 h_1}{2} \right) \right] \left[ 1 + \frac{4\tilde{\mu}_n}{h_2^2} \sin^2 \left( \frac{\tilde{\eta}_2 h_2}{2} \right) \right] \right|} \leq 1, \quad \forall n \geq 1. \quad (2.92)$$

*Lemma 2.4.2.* Suppose that  $\zeta^n$ ,  $1 \leq n \leq N$  are the solutions of equation (2.90), then

$$|\zeta^n| \leq |\zeta^0|, \quad 1 \leq n \leq N. \quad (2.93)$$

*Proof.* By mathematical induction, we prove this Lemma. If  $n = 1$ , equation (2.91) converts to

$$\zeta^1 \leq \frac{(1 + \tilde{\mu}_1 a_1^{(1)})(1 + AB)}{(1 + A)(1 + B)} \zeta^0 \leq \frac{(1 + AB)}{(1 + A)(1 + B)} \zeta^0. \quad (2.94)$$

It can be easily observed that

$$F(1) = \frac{2^{\alpha-1}}{\Gamma(3-\alpha)} \tau_1^{1-\alpha} > 0, \quad \tilde{\mu}_1 > 0, \quad a_1^{(1)} > 0.$$

Using the Lemma 2.4.1 and above inequalities, we have

$$|\zeta^1| \leq |\zeta^0|. \quad (2.95)$$

Now suppose that

$$|\zeta^n| \leq |\zeta^0|, \quad n = 1, 2, \dots, r - 1. \quad (2.96)$$

By setting  $n = r$  in equation (2.91) and then using the equation (2.19) and (2.96), we obtain

$$|\zeta^r| \leq |\zeta^0|. \quad (2.97)$$

This completes the proof.  $\square$

## 2.4.2 Stability Analysis for the Nonuniform Crank-Nicolson $L1 - 2$ Difference Scheme

Substituting the approximation of TFCD (2.27) and spatial derivatives approximation (2.47) into the equation (2.1)-(2.3), we obtain the following system of equations,

$$\left\{ \begin{array}{l} d_0^{(n)} \delta_t u_{i,j}^{n-\frac{1}{2}} - \sum_{k=1}^{n-1} (d_{n-k-1}^{(n)} - d_{n-k}^{(n)}) u_{i,j}^{k-\frac{1}{2}} - d_{n-1}^{(n)} v^0 \\ \quad = \Delta_h u_{i,j}^{n-\frac{1}{2}} + f_{i,j}^{n-\frac{1}{2}} + r^{n-\frac{1}{2}}, \quad 1 \leq n \leq N, \\ u_{i,j}^n = \Phi(x_i, y_j, t_n), \quad (x_i, y_j) \in \Omega_s, \quad t \in (0, T], \\ u_{i,j}^0 = \phi(x_i, y_j), \quad v_{i,j}^0 = \varphi(x_i, y_j), \quad (x_i, y_j) \in \bar{\Omega}_s. \end{array} \right. \quad (2.98)$$

Suppose

$$\Theta_{i,j}^n = U_{i,j}^n - u_{i,j}^n, \quad 1 \leq i \leq M_1 - 1, \quad 1 \leq j \leq M_2 - 1, \quad n \geq 1, \quad (2.99)$$

where,  $U_{i,j}^n$  be the numerical solution of model (2.1)-(2.3) and  $u_{i,j}^n$  be the exact solution of difference scheme (2.98). Now, using the equation (2.99) in (2.98)

$$\begin{aligned} \frac{d_0^{(n)}}{\tau_n}(\Theta_{i,j}^n - \Theta_{i,j}^{n-1}) - \sum_{k=1}^{n-1} \frac{d_{n-k-1}^{(n)} - d_{n-k}^{(n)}}{\tau_k}(\Theta_{i,j}^k - \Theta_{i,j}^{k-1}) &= \frac{1}{\tau_n} \Delta_h(\Theta_{i,j}^n - \Theta_{i,j}^{n-1}), \\ d_0^{(n)} \Theta_{i,j}^n &= d_0^{(n)} \Theta_{i,j}^{n-1} + \tau_n \sum_{k=1}^{n-1} \frac{d_{n-k-1}^{(n)} - d_{n-k}^{(n)}}{\tau_k}(\Theta_{i,j}^k - \Theta_{i,j}^{k-1}) + \Delta_h(\Theta_{i,j}^n - \Theta_{i,j}^{n-1}). \end{aligned} \quad (2.100)$$

Suppose the solution of equation (2.100) is  $\Theta_{i,j}^n = \zeta^n e^{\iota(i\tilde{\eta}_1 h_1 + j\tilde{\eta}_2 h_2)}$ , by using the idea as in the previous stability theorem, we have

$$\begin{aligned} d_0^{(n)} \zeta^n &= d_0^{(n)} \zeta^{n-1} + \tau_n \sum_{k=1}^{n-1} \frac{d_{n-k-1}^{(n)} - d_{n-k}^{(n)}}{\tau_k}(\zeta^k - \zeta^{k-1}) - 4 \left[ \frac{1}{h_1^2} \sin^2 \left( \frac{\tilde{\eta}_1 h_1}{2} \right) \right. \\ &\quad \left. + \frac{1}{h_2^2} \sin^2 \left( \frac{\tilde{\eta}_2 h_2}{2} \right) \right] \zeta^n + 4 \left[ \frac{1}{h_1^2} \sin^2 \left( \frac{\tilde{\eta}_1 h_1}{2} \right) + \frac{1}{h_2^2} \sin^2 \left( \frac{\tilde{\eta}_2 h_2}{2} \right) \right] \zeta^{n-1}, \\ (d_0^{(n)} + C + D) \zeta^n &= (d_0^{(n)} + C + D) \zeta^{n-1} + \tau_n \sum_{k=1}^{n-1} \frac{d_{n-k-1}^{(n)} - d_{n-k}^{(n)}}{\tau_k}(\zeta^k - \zeta^{k-1}), \end{aligned} \quad (2.101)$$

where

$$C = \frac{4}{h_1^2} \sin^2 \left( \frac{\tilde{\eta}_1 h_1}{2} \right) \geq 0, \quad D = \frac{4}{h_2^2} \sin^2 \left( \frac{\tilde{\eta}_2 h_2}{2} \right) \geq 0. \quad (2.102)$$

By using the equation (2.102) and Lemma 2.2.4, we have

$$|\zeta^n| = \left| \frac{(d_0^{(n)} + C + D) \zeta^{n-1} + \tau_n \sum_{k=1}^{n-1} \frac{d_{n-k-1}^{(n)} - d_{n-k}^{(n)}}{\tau_k}(\zeta^k - \zeta^{k-1})}{(d_0^{(n)} + C + D)} \right| \leq |\zeta^{n-1}|, \quad \forall n \geq 3. \quad (2.103)$$

Therefore, we have  $|\zeta^n| \leq |\zeta^0|$ .

## 2.5 The Derivation of the Nonuniform Difference Schemes for One-Dimensional Case

Using the approximation of TFCD from equations (2.7) and (2.22), and central difference approximation of second order spatial derivative,

$$\frac{\partial^2 u(x_i, t_n)}{\partial x^2} = \frac{u_{i+1}^n - 2u_i^n + u_{i-1}^n}{h^2} + \mathcal{O}(h^2),$$

we obtain the following schemes for 1D case:

### 2.5.1 Nonuniform $L1$ Difference Scheme

$$\left\{ \begin{array}{l} a_1^{(n)} \left\{ \frac{U_i^n - U_i^{n-1}}{\tau_n} \right\} + \sum_{k=1}^{n-1} (a_{n-k+1}^{(n)} - a_{n-k}^{(n)}) \left\{ \frac{U_i^k - U_i^{k-1}}{\tau_k} \right\} + F(n) \left\{ \frac{U_i^n - U_i^{n-1}}{\tau_n} \right. \\ \left. - \frac{U_i^{n-1} - U_i^{n-2}}{\tau_{n-1}} \right\} - a_n^{(n)} v_i^0 = \frac{U_{i+1}^n - 2U_i^n + U_{i-1}^n}{h^2} + f_i^n, \quad 1 \leq i \leq M-1, \quad 1 \leq n \leq N, \\ U_i^n = \Phi(x_i, t_n), \quad 1 \leq i \leq M-1, \quad 1 \leq n \leq N, \\ U_i^0 = \phi(x_i), \quad \frac{\partial U}{\partial t} \Big|_{t=0} = \varphi(x_i), \quad 0 \leq i \leq M, \end{array} \right. \quad (2.104)$$

where  $F(n) = \frac{2^{\alpha-1}}{\Gamma(3-\alpha)} \frac{\tau_n^{2-\alpha}}{(\tau_{n-1} + \tau_n)}$ ,  $n \geq 2$ , and  $F(1) = \frac{2^{\alpha-1}}{\Gamma(3-\alpha)} \tau_1^{1-\alpha}$ .

### 2.5.2 Nonuniform Crank-Nicolson $L1 - 2$ Difference Scheme

$$\left\{ \begin{array}{l} \frac{\tau_1^{1-\alpha}}{2^{2-\alpha} \Gamma(3-\alpha)} (V_i^1 - V_i^0) = \delta_x^2 U_i^{\frac{1}{2}} + f_i^{\frac{1}{2}}, \quad 1 \leq i \leq M-1, \\ \frac{\tau_1^{1-\alpha}}{2^{2-\alpha} \Gamma(3-\alpha)} (V_i^1 - V_i^0) + \frac{(\tau_1 + \tau_2)^{1-\alpha}}{2^{2-\alpha} \Gamma(3-\alpha)} (V_i^2 - V_i^0) = \delta_x^2 U_i^{\frac{3}{2}} + f_i^{\frac{3}{2}}, \quad 1 \leq i \leq M-1, \\ d_0^{(n)} \frac{V_i^n + V_i^{n-1}}{2} - \sum_{k=1}^{n-1} (d_{n-k-1}^{(n)} - d_{n-k}^{(n)}) \frac{V_i^k + V_i^{k-1}}{2} - d_{n-1}^{(n)} V_i^0 = \delta_x^2 U_i^{n-\frac{1}{2}} + f_i^{n-\frac{1}{2}}, \quad n \geq 3, \\ V_i^{n-\frac{1}{2}} = \delta_t U_i^{n-\frac{1}{2}}, \quad 1 \leq i \leq M-1, \quad 1 \leq n \leq N, \\ U_i^n = \Phi(x_i t_n), \quad 1 \leq i \leq M-1, \quad 1 \leq n \leq N, \\ U_i^0 = \phi(x_i), \quad \frac{\partial U}{\partial t} \Big|_{t=0} = \varphi(x_i), \quad 0 \leq i \leq M. \end{array} \right. \quad (2.105)$$

## 2.6 Numerical Results

In this section, we present two numerical examples of the considered problem (2.1)-(2.3) to verify theoretical results. Here, we have some cases for the exact solution  $u$  of the problem (2.1) according to the regularity conditions (R1 and R2-R4). We use uniform meshes for those cases that satisfy the regularity conditions, and if there is a strong singularity at  $t = 0$ , then we use nonuniform mesh to achieve the theoretical convergence order. In first example, we solve 1D TFDW equation using the difference schemes (2.104) and (2.105) with smooth and non-smooth exact solution. We take 2D TFDW equation in the second example to test the accuracy of difference schemes defined in (2.56)-(2.59) and (2.74)-(2.80).

*Example 2.6.1.* Consider the TFDW equation (2.1)-(2.3) with the domain  $(x, t) \in (0, 1) \times (0, 1]$ .

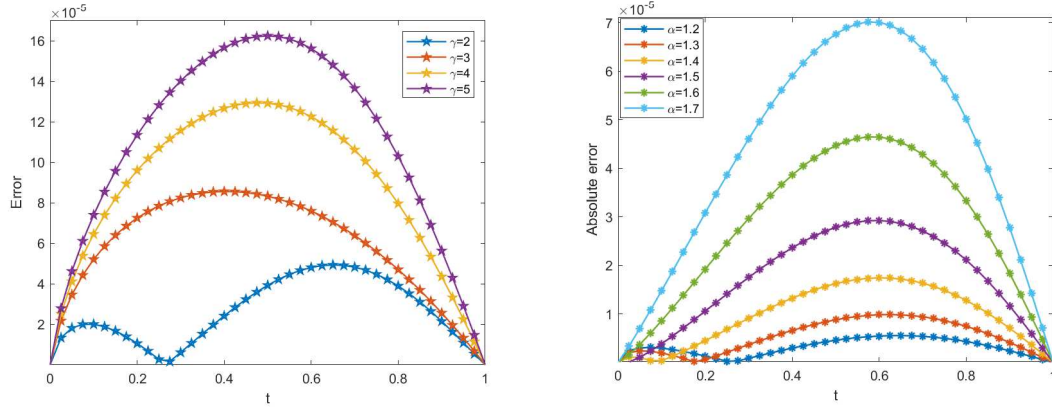
For  $f(x, t) = \omega_{1+\rho-\alpha}x^{1+\alpha}(1-x) + (1+\alpha)((\alpha+2)x-\alpha)x^{\alpha-1}\omega_{1+\rho}(t)$ , the exact solution of the considered problem (2.1) is  $u(x, t) = \omega_{1+\rho}(t)x^{1+\alpha}(1-x)$  with initial and boundary conditions  $\Phi = 0$ ,  $\phi = 0$ ,  $\varphi = 0$ . Now, we take different choices of the function through  $\rho$  according to regularity conditions. Numerical results for the scheme (2.104) are discussed in Tables 2.3-2.7 and for the scheme (2.105) in Tables 2.8-2.11.

In Tables 2.3, 2.4, 2.5, we give the maximum absolute error and OC in the time direction for fixed  $h = \frac{1}{1000}$  and different choices of  $\alpha = 1.25, 1.5, 1.85$  with the cases  $\rho = (2+\alpha)$ ,  $\rho = (1+\alpha)$ ,  $\rho = \alpha$ , respectively. Table 2.3 is defined for  $\gamma = 1$  (uniform meshes), and in Table 2.4 and Table 2.5, we use nonuniform mesh with  $\gamma = 1.5, 3, 4$  to get the desired accuracy.

TABLE 2.3: Temporal numerical results for the scheme (2.104) with  $\gamma = 1$ ,  $\rho = (2+\alpha)$  and  $M = 1000$ .

$\tau$	$\alpha = 1.85$		$\alpha = 1.5$		$\alpha = 1.25$	
	$\ u^\tau - U^\tau\ _\infty$	OC	$\ u^\tau - U^\tau\ _\infty$	OC	$\ u^\tau - U^\tau\ _\infty$	OC
$1/2^5$	1.5551E-04		4.6595E-05		1.6884E-05	
$1/2^6$	7.1611E-05	1.1188	1.6536E-05	1.4946	4.9907E-06	1.7583
$1/2^7$	3.2623E-05	1.1343	5.8672E-06	1.4948	1.4777E-06	1.7558
$1/2^8$	1.4780E-05	1.1422	2.0776E-06	1.4978	4.3455E-07	1.7658
$1/2^9$	6.6768E-06	1.1464	7.3218E-07	1.5046	1.2409E-07	1.8081
$1/2^{10}$	3.0109E-06	1.1490	2.5497E-07	1.5218	3.4379E-08	1.8518

In Figure 2.3, plot 2.3(a) shows the effect of mesh grading parameters  $\gamma$ 's on the absolute error for a non-smooth exact solution as taking  $\rho = \alpha$ . We take a particular  $\alpha = 1.5$  and different  $\gamma = 2, 3, 4, 5$  with  $M = N = 40$ . Plot 2.3(b) shows the behavior of absolute error on uniform mesh ( $\gamma = 1$ ) for a sufficiently smooth exact solution as taking  $\rho = (2+\alpha)$  with  $M = N = 40$ .



(a) Scheme (2.104) for  $\rho = \alpha$  with  $\alpha = 1.5$ .      (b) Scheme (2.104) for  $\rho = (2 + \alpha)$  with  $\gamma = 1$ .

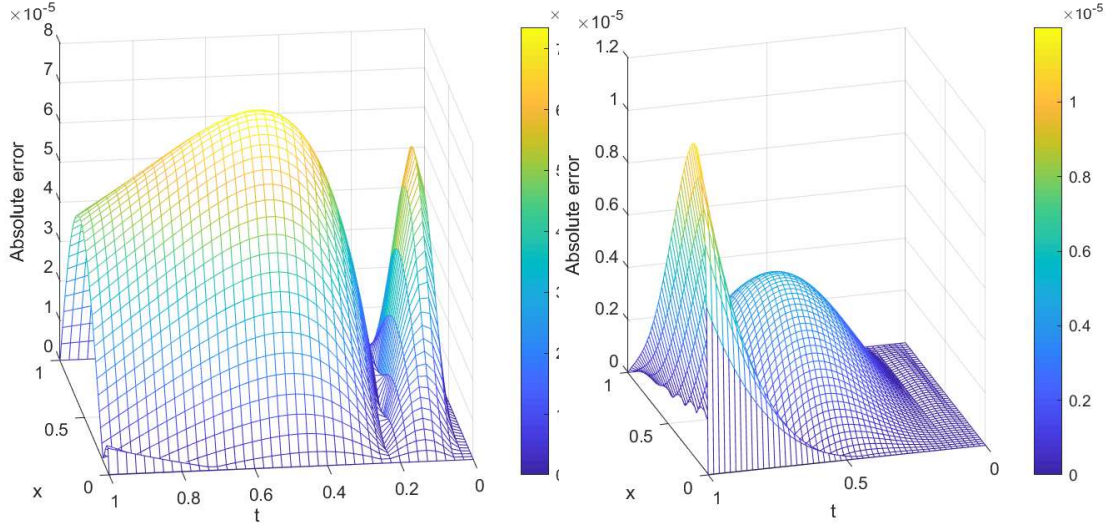
FIGURE 2.3: Plot of the absolute error for different choices of  $\gamma$  (Left side (a)) and for different values of  $\alpha$  (Right side (b)).

TABLE 2.4: Temporal numerical results for the scheme (2.104) with different  $\gamma$ ,  $\rho = (1 + \alpha)$  and  $M = 1000$ .

$\tau$	$\alpha = 1.85, \gamma = 1$		$\alpha = 1.25, \gamma = 1$		$\alpha = 1.25, \gamma = 1.5$	
	$\ u^\tau - U^\tau\ _\infty$	OC	$\ u^\tau - U^\tau\ _\infty$	OC	$\ u^\tau - U^\tau\ _\infty$	OC
$1/2^5$	2.3185E-04		8.5477E-05		3.0096E-05	
$1/2^6$	1.0840E-04	1.0968	3.6626E-05	1.2227	8.8478E-06	1.7662
$1/2^7$	4.9818E-05	1.1216	1.5737E-05	1.2187	2.5666E-06	1.7854
$1/2^8$	2.2675E-05	1.1355	6.7302E-06	1.2254	7.3578E-07	1.8025
$1/2^9$	1.0266E-05	1.1432	2.8585E-06	1.2354	2.0920E-07	1.8144
$1/2^{10}$	4.6336E-06	1.1477	1.2070E-06	1.2439	5.8863E-08	1.8294

Figures 2.4 and 2.6 display the behavior of the uniform and nonuniform meshes near singularity at  $t = 0$ . In graphs 2.4(a) and 2.6(a), we represent the absolute error by using  $\gamma = 1$ ,  $\alpha = 1.2$ ,  $T = 1$  for cases  $\rho = (1 + \alpha)$  and  $\rho = \alpha$  for Example 2.6.1, respectively. The graphs 2.4(b) and 2.6(b) show the same error but for the nonuniform meshes by taking  $(\rho, \gamma) = (1 + \alpha, 2)$  and  $(\rho, \gamma) = (\alpha, 4)$ , respectively.

From the figures 2.4(a) and 2.6(a), we can see that the error blows-up near the singularity  $t = 0$  after that it decreases smoothly. To handle such behavior of error, we take nonuniform mesh by selecting  $\gamma = 2$ ,  $\gamma = 4$  and display the absolute errors in the figures 2.4(b) and 2.6(b), respectively.

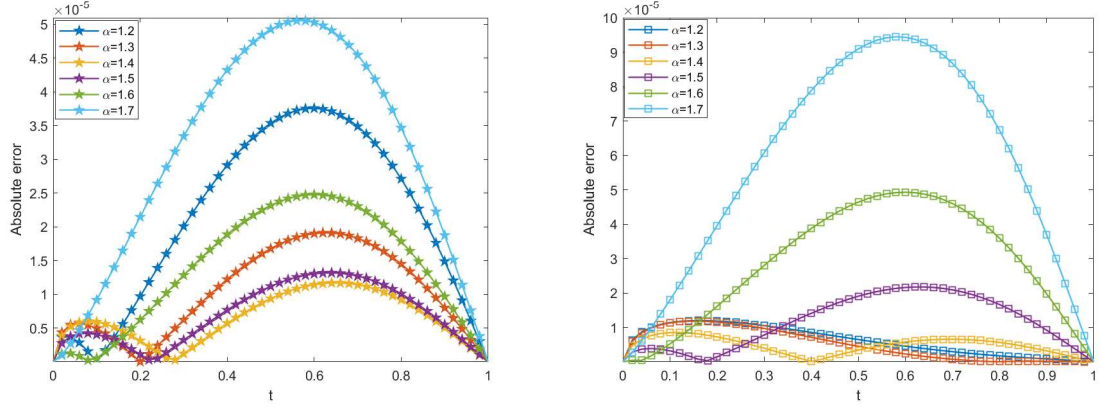


(a) Scheme (2.104) with  $\gamma = 1$  and  
 $\alpha = 1.2$

(b) Scheme (2.104) with  $\gamma = 2$  and  
 $\alpha = 1.2$

FIGURE 2.4: Absolute error for the case  $\rho = (1 + \alpha)$  on the uniform and nonuniform meshes with  $M = N = 50$ .

In Figures 2.5 and 2.7, we compare the maximum absolute error between uniform mesh ( $\gamma = 1$ ) and nonuniform mesh ( $\gamma = 2$  for 2.5(b) and  $\gamma = 4$  for 2.7(b)) when  $\alpha = 1.2$  and  $T = 1$ . Figures 2.5 and 2.7 represent the absolute error for the Example 2.6.1 for  $\rho = (1 + \alpha)$  and  $\rho = \alpha$ , respectively. One can note from these figures that the error behavior near the singularity point  $t = 0$ , also the error decreases for choice of nonuniform mesh in approximation method.



(a) Scheme (2.104) with  $\rho = (1 + \alpha)$  and (b) Scheme (2.104) with  $\rho = (1 + \alpha)$  and

$$\gamma = 1$$

$$\gamma = 2.$$

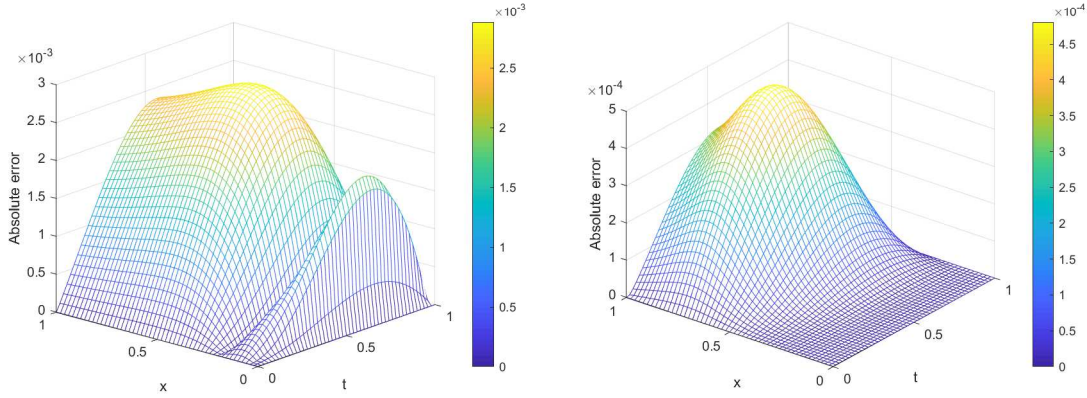
FIGURE 2.5: Comparison of uniform and nonuniform meshes for the absolute error in Example 2.6.1 with  $\rho = (1 + \alpha)$ ,  $M = N = 50$ .

TABLE 2.5: Temporal numerical results for the scheme (2.104) with  $\rho = \alpha$ , and  $M = 1000$ .

$\tau$	$\alpha = 1.5, \gamma = 1$		$\alpha = 1.5, \gamma = 3$		$\alpha = 1.5, \gamma = 4$	
	$\ u^\tau - U^\tau\ _\infty$	OC	$\ u^\tau - U^\tau\ _\infty$	OC	$\ u^\tau - U^\tau\ _\infty$	OC
$1/2^5$	1.5779E-03		9.0421E-05		1.7619E-04	
$1/2^6$	6.9573E-04	1.1814	2.7519E-05	1.7162	6.5481E-05	1.4280
$1/2^7$	4.5687E-04	0.6067	9.1531E-06	1.5881	2.4027E-05	1.4464
$1/2^8$	3.4197E-04	0.4179	3.1692E-06	1.5301	8.7233E-06	1.4617
$1/2^9$	2.6153E-04	0.3869	1.1181E-06	1.5031	3.1491E-06	1.4699
$1/2^{10}$	1.9926E-04	0.3923	4.0036E-07	1.4816	1.1362E-06	1.4707

Table 2.6 indicates the comparison of our scheme (2.104) and the scheme defined in [1] for Example 1 of [1]. In this Table 2.6, we set  $h = \frac{1}{1000}$  and display the temporal OC for  $\alpha = 1.1$  and 1.5. Table 2.6 confirms that the proposed scheme (2.104) is computationally efficient and agrees with the theoretical convergence order. We can see from Table 2.6 that the temporal accuracy of the current scheme (2.104) agrees

with  $\min(3 - \alpha, \gamma\alpha)$ . Table 2.6 also represents that the proposed scheme is stable as the order remain unchanged up to two decimal places.



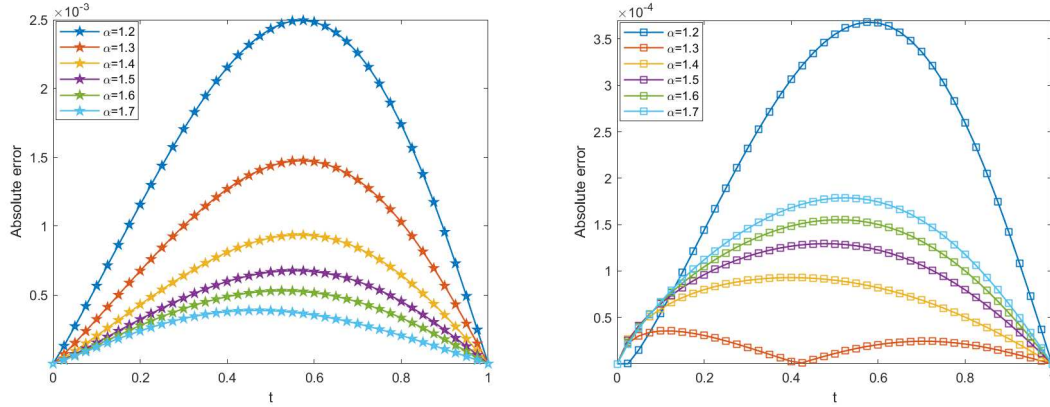
(a) Scheme (2.104) with  $\gamma = 1$  and  $\alpha = 1.2$ .

(b) Scheme (2.104) with  $\gamma = 4$  and  $\alpha = 1.2$ .

FIGURE 2.6: Absolute error graphs for  $\rho = \alpha$  in Example 2.6.1 on the uniform (a) and nonuniform (b) meshes with  $M = N = 50$ .

TABLE 2.6: Temporal numerical results for Example 1 of [1] using the scheme (2.104) and scheme defined in [1] with different  $\alpha$  and  $M = 1000$ .

	$\alpha = 1.1$			$\alpha = 1.5$		
	Current scheme	OC	Scheme[1]	Current scheme	OC	Scheme [1]
$\tau$	$\ u^\tau - U^\tau\ _\infty$	OC	OC	$\ u^\tau - U^\tau\ _\infty$	OC	OC
1/20	1.2745E-03			6.7126E-03		
1/40	3.3928E-04	1.9094	1.8783	2.3565E-03	1.5102	1.5143
1/80	9.0394E-05	1.9082	1.8722	8.2747E-04	1.5099	1.5056
1/160	2.4092E-05	1.9077	1.8479	2.9071E-04	1.5091	1.4998
Theoretical OC ( $3 - \alpha$ )		1.90			1.50	



(a) Scheme (2.104) for case  $\rho = \alpha$  with  $\gamma = 1$ . (b) Scheme (2.104) for case  $\rho = \alpha$  with  $\gamma = 4$ .

FIGURE 2.7: Comparison of uniform and nonuniform meshes for the absolute error in Example 2.6.1 with  $\rho = \alpha$ ,  $M = N = 50$ .

TABLE 2.7: Spatial numerical results for the scheme (2.104) with  $\alpha = 1.5$ , and  $N = 1000$ .

$h$	$\rho = (2 + \alpha), \gamma = 1$		$\rho = (1 + \alpha), \gamma = 2$		$\rho = \alpha, \gamma = 3$	
	$\ u^\tau - U^\tau\ _\infty$	OC	$\ u^\tau - U^\tau\ _\infty$	OC	$\ u^\tau - U^\tau\ _\infty$	OC
1/8	1.1787E-04		5.0905E-04		1.5865E-03	
1/16	3.1292E-05	1.9133	1.3328E-04	1.9333	4.1504E-04	1.9345
1/32	7.9772E-06	1.9718	3.4240E-05	1.9607	1.0684E-04	1.9579
1/64	1.9214E-06	2.0538	8.5390E-06	2.0036	2.7290E-05	1.9690

In Tables 2.8, 2.9 and 2.10, we express the maximum absolute error and OC in temporal direction using the scheme (2.105) for Example 2.6.1. We take fixed  $h = \frac{1}{1000}$  and different choices of  $\alpha = 1.25, 1.35, 1.5, 1.55, 1.75, 1.9$  varying  $\rho = (3 + \alpha)$ ,  $\rho = (2 + \alpha)$ ,  $\rho = (1 + \alpha)$ , respectively. This scheme (2.105) gives better temporal accuracy as compared to the existing works [64], [79], [76], [123] for the TFDWE with second-order temporal accuracy. Table 2.11 shows the maximum error and OC in space direction by taking fixed  $M = 1000$  for the Example 2.6.1. We present the

numerical results for the  $\alpha = 1.5$  with different choices of pair  $(\rho, \gamma) = (3 + \alpha, 1)$ ,  $(\rho, \gamma) = (2 + \alpha, 1.1)$ ,  $(\rho, \gamma) = (1 + \alpha, 1.15)$ .

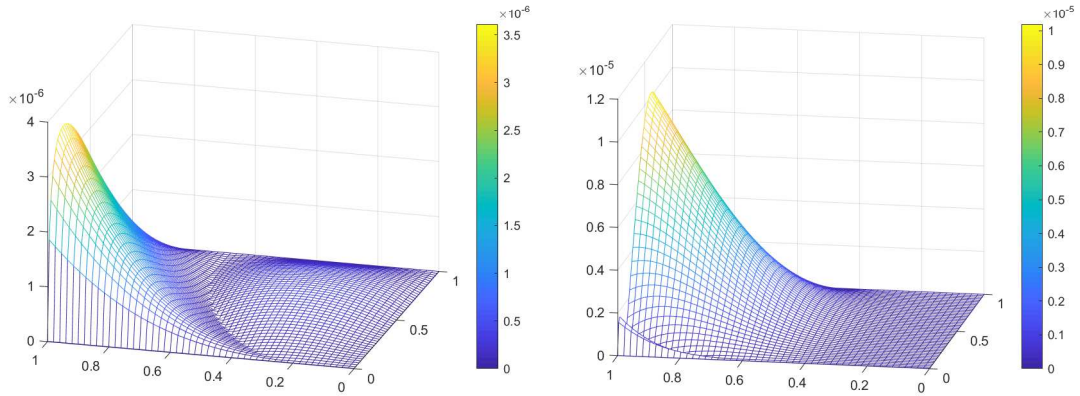
TABLE 2.8: Temporal numerical results for scheme (2.105) for  $\rho = (3 + \alpha)$ , and  $M = 1000$ .

$\tau$	$\alpha = 1.9$		$\alpha = 1.5$		$\alpha = 1.25$	
	$\ u^\tau - U^\tau\ _\infty$	OC	$\ u^\tau - U^\tau\ _\infty$	OC	$\ u^\tau - U^\tau\ _\infty$	OC
$1/2^3$	3.7079E-05		2.0106E-05		1.5922E-05	
$1/2^4$	9.4946E-06	1.9654	4.5280E-06	2.1507	3.7714E-06	2.0779
$1/2^5$	2.3324E-06	2.0253	1.0332E-06	2.1317	9.0759E-07	2.0550
$1/2^6$	5.6308E-07	2.0504	2.3907E-07	2.1117	2.2027E-07	2.0428
$1/2^7$	1.3469E-07	2.0637	5.5497E-08	2.1069	5.3046E-08	2.0540
$1/2^8$	3.1834E-08	2.0810	1.2366E-08	2.1660	1.1991E-08	2.1452

TABLE 2.9: Temporal numerical results for scheme (2.105) for  $\rho = (2 + \alpha)$ , and  $M = 1000$ .

$\tau$	$\alpha = 1.9$		$\alpha = 1.5$		$\alpha = 1.25$	
	$\ u^\tau - U^\tau\ _\infty$	OC	$\ u^\tau - U^\tau\ _\infty$	OC	$\ u^\tau - U^\tau\ _\infty$	OC
$1/2^3$	6.9430E-05		2.9153E-05		2.0756E-05	
$1/2^4$	1.6753E-05	2.0512	6.2321E-06	2.2258	4.5763E-06	2.1813
$1/2^5$	3.9882E-06	2.0706	1.3839E-06	2.1709	1.0824E-06	2.0800
$1/2^6$	9.4776E-07	2.0732	3.1744E-07	2.1242	2.6325E-07	2.0397
$1/2^7$	2.2450E-07	2.0778	7.4361E-08	2.0939	6.4576E-08	2.0274
$1/2^8$	5.2424E-08	2.0984	1.7441E-08	2.0920	1.5736E-08	2.0369

Figure 2.8 displays the absolute error for Example 2.6.1 for the case  $\rho = (1 + \alpha)$  using the scheme (2.105) at the final time  $T = 1$ . The graphs 2.8(a) and 2.8(b) show the same error for  $\alpha = 1.2$ ,  $M = N = 50$  with  $\gamma = 1$  and  $\gamma = 2$ , respectively.



(a) Scheme (2.105) with  $\gamma = 1$  and  $\alpha = 1.2$ .      (b) Scheme (2.105) with  $\gamma = 2$  and  $\alpha = 1.2$ .

FIGURE 2.8: Absolute error graphs for the case  $\rho = (1 + \alpha)$  in Example 2.6.1 on the uniform (a) and nonuniform (b) meshes with  $M = N = 50$ .

TABLE 2.10: Temporal numerical results of the scheme (2.105) for  $\rho = (1 + \alpha)$ , and  $M = 1000$ .

$\tau$	$\alpha = 1.35$		$\alpha = 1.55$		$\alpha = 1.75$	
	$\ u^\tau - U^\tau\ _\infty$	OC	$\ u^\tau - U^\tau\ _\infty$	OC	$\ u^\tau - U^\tau\ _\infty$	OC
$1/2^3$	6.6715E-05		8.8646E-05		1.2153E-04	
$1/2^4$	1.6155E-05	2.0460	2.2324E-05	1.9895	3.1289E-05	1.9576
$1/2^5$	4.0502E-06	1.9959	5.2837E-06	2.0789	7.5279E-06	2.0553
$1/2^6$	9.1518E-07	2.1459	1.2140E-06	2.1218	1.7716E-06	2.0872
$1/2^7$	2.1263E-07	2.1057	2.8309E-07	2.1004	4.1671E-07	2.0879
$1/2^8$	5.1874E-08	2.0353	6.7074E-08	2.0774	9.8436E-08	2.0818

Figure 2.9 shows the maximum absolute error for the Example 2.6.1 for  $\rho = (1 + \alpha)$  with uniform meshes using the different values of  $\alpha$  and final time  $T = 1$ . We can see from Figures 2.5(a) and (2.9) that both the schemes (2.104) and (2.105) have different behavior near the singular point  $t = 0$ .

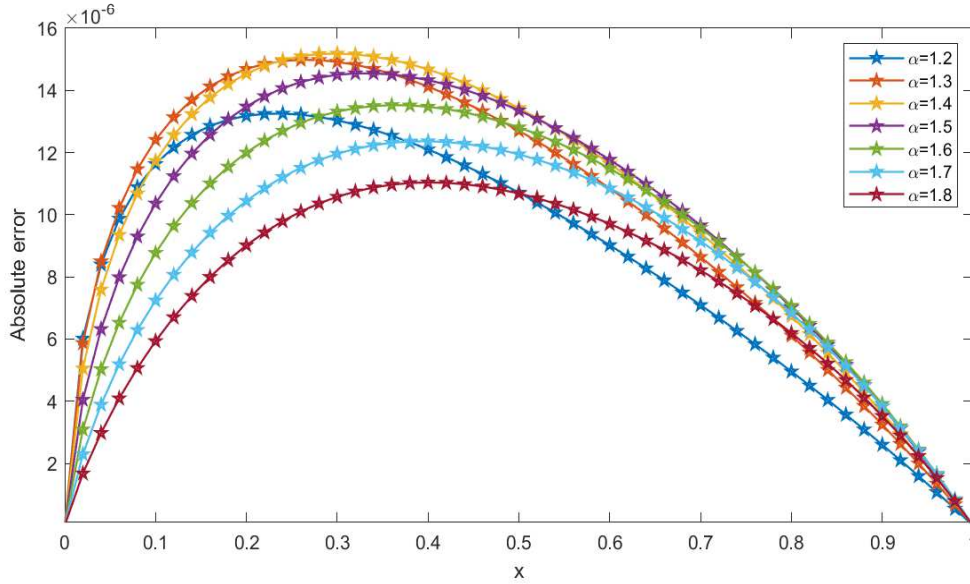


FIGURE 2.9: Absolute error plot for the case  $\rho = (1 + \alpha)$  in Example 2.6.1 by using scheme (2.105) with  $\gamma = 1$  and  $M = N = 50$ .

TABLE 2.11: Spatial numerical results for the scheme (2.105) with  $\alpha = 1.5$ , and  $N = 1000$ .

$h$	$\rho = (3 + \alpha), \gamma = 1$		$\rho = (2 + \alpha), \gamma = 1.1$		$\rho = (1 + \alpha), \gamma = 1.15$	
	$\ u^\tau - U^\tau\ _\infty$	OC	$\ u^\tau - U^\tau\ _\infty$	OC	$\ u^\tau - U^\tau\ _\infty$	OC
1/8	2.2189E-05		1.1829E-04		5.0706E-04	
1/16	5.9343E-06	1.9027	3.1472E-05	1.9101	1.3272E-04	1.9337
1/32	1.5463E-06	1.9402	8.0905E-06	1.9598	3.4047E-05	1.9628
1/64	3.9685E-07	1.9622	2.0130E-06	2.0069	8.4406E-06	2.0121

*Example 2.6.2.* [79] Consider Eq. (2.1)-(2.3) with domain  $\Omega = (0, \pi) \times (0, \pi) \times (0, 1)$ .

For  $f(x, y, t) = (\omega_{1+\rho-\alpha}(t) + 2\omega_{1+\rho}(t)) \sin(x) \sin(y)$ , the exact solution of considered problem is  $u(x, y, t) = \omega_{1+\rho}(t) \sin(x) \sin(y)$  with initial-boundary conditions  $\Phi(x, y, t) = 0$ ,  $\phi(x, y) = 0$ ,  $\varphi(x, y) = 0$ .

Table 2.12 and 2.13 show the numerical results for Example 2.6.2 using the Nonuniform  $L1$  scheme defined in (2.56)-(2.59) with the uniform mesh (for smooth solution)

and nonuniform mesh (for nonsmooth solution). Table 2.12 represents the maximum absolute error and OC in space direction for different values of  $M_1 = M_2$  and fixed  $N = 20,000$ . One can note from Table 2.12 that the spatial accuracy is second-order. Table 2.13 displays the maximum absolute error and OC in temporal direction for various values of  $N$  and fixed space step sizes  $h_1 = h_2 = \frac{\pi}{50}$ . From Table 2.13, we can see that the OC in the time direction is  $\min(3 - \alpha, \gamma\alpha)$ .

TABLE 2.12: Spatial numerical results of the scheme (2.56)-(2.59) for Example 2.6.2 with  $\alpha = 1.5$ , and  $N = 20,000$ .

$M$	$(\rho, \gamma)$	$\alpha = 1.45$		$\alpha = 1.65$		$\alpha = 1.65$
		$\ u^\tau - U^\tau\ _\infty$	OC	$\ u^\tau - U^\tau\ _\infty$	OC	CPU (sec)
4	$(2 + \alpha, 1)$	8.7071E-04		4.5982E-04		4075.239806
8		2.1998E-04	1.9848	1.1664E-04	1.9790	8621.444199
16		5.5178E-05	1.9952	2.9529E-05	1.9819	16060.70875
32		1.3846E-05	1.9946	7.6680E-06	1.9452	33236.43620
4	$(1 + \alpha, 1.2)$	4.1046E-03		2.3745E-03		4115.529557
8		1.0353E-03	1.9871	6.0080E-04	1.9827	8661.684593
16		2.5947E-04	1.9965	1.5111E-04	1.9913	15959.27646
32		6.4965E-05	1.9978	3.8299E-05	1.9803	33704.99553
4	$(\alpha, 4)$	1.5026E-02		4.1046E-03		4110.386096
8		3.7806E-03	1.9908	1.0353E-03	1.9871	8689.546216
16		9.4646E-04	1.9980	2.5947E-04	1.9965	16193.19899
32		2.3651E-04	2.0006	6.4965E-05	1.9978	33256.90475

TABLE 2.13: Temporal numerical results for the scheme (2.56)-(2.59) for Example 2.6.2 with  $h_1 = h_2 = \frac{\pi}{50}$ .

$\tau$	$(\rho, \gamma)$	$\alpha = 1.45$		$\alpha = 1.65$		$\alpha = 1.85$	
		$\ u^\tau - U^\tau\ _\infty$	OC	$\ u^\tau - U^\tau\ _\infty$	OC	$\ u^\tau - U^\tau\ _\infty$	OC
1/10	$(2 + \alpha, 1)$	6.5913E-03		9.5029E-03		1.2914E-02	
1/20		2.3730E-03	1.4738	3.9215E-03	1.2770	5.9396E-03	1.1205
1/40		8.3471E-04	1.5074	1.5840E-03	1.3078	2.7080E-03	1.1332
1/80		2.9278E-04	1.5115	6.3339E-04	1.3224	1.2297E-03	1.1389
1/10	$(1 + \alpha, 1.2)$	1.4813E-02		2.0292E-02		3.1465E-02	
1/20		5.2452E-03	1.4978	8.0702E-03	1.3302	1.4324E-02	1.1353
1/40		1.7837E-03	1.5561	3.1326E-03	1.3652	6.4405E-03	1.1532
1/80		6.0780E-04	1.5532	1.2160E-03	1.3653	2.8939E-03	1.1541
1/10	$(\alpha, 4)$	2.7839E-02		4.6682E-02		3.5147E-02	
1/20		7.8851E-03	1.8199	1.7407E-02	1.4232	1.3946E-02	1.3336
1/40		2.6839E-03	1.5548	6.8804E-03	1.3391	6.2221E-03	1.1644
1/80		9.1602E-04	1.5509	2.6719E-03	1.3646	2.7662E-03	1.1695

Let  $h_1 = h_2 = h$  be the spatial step-sizes. We use the following formula to compute the error of the numerical solution with the exact solution

$$E(h, \tau) = \max_{\substack{1 \leq i \leq M_1 - 1 \\ 1 \leq j \leq M_2 - 1}} \|U(x_i, y_j, t_N) - u(x_i, y_j, t_N)\|_\infty,$$

where  $U(x_i, y_j, t_N)$  and  $u(x_i, y_j, t_N)$  denotes the approximate and exact solutions of the problem (2.1) at the final time  $T = 1$ . We use the following formulas to find the convergence order in temporal and spatial direction for the proposed ADI schemes (2.56)-(2.59) and (2.74)-(2.80) corresponding to the maximum norm.

$$r_t = \log_2 \left( \frac{E(h, 2\tau)}{E(h, \tau)} \right), \quad r_s = \log_2 \left( \frac{E(2h, \tau)}{E(h, \tau)} \right).$$

Table 2.14 and 2.15, presents the maximum absolute error and corresponding OC in spatial and time directions, respectively, for Example 2.6.2 with different  $\rho = (4 + \alpha)$ ,  $(3 + \alpha)$ ,  $(2 + \alpha)$ . For Table 2.14, we set a fixed time step size  $\tau = 1/20000$  and vary the values of  $M_1 = M_2$ . We can note from Table 2.14 that the Nonuniform Crank-Nicolson difference scheme (2.74)-(2.80) is second-order accurate in space. In Table 2.15, we compute the absolute error for keeping fixed  $h_1 = h_2 = \frac{\pi}{50}$  and different values of  $N$ . We can remark from Table 2.15 that the OC in the temporal direction for the scheme (2.74)-(2.80) is second.

TABLE 2.14: Spatial numerical results of Example 2.6.2 for the scheme (2.74)-(2.80) with  $\gamma = 1$ , and  $N = 20,000$ .

$M$	$\rho$	$\alpha = 1.45$		$\alpha = 1.65$		$\alpha = 1.65$
		$\ u^\tau - U^\tau\ _\infty$	OC	$\ u^\tau - U^\tau\ _\infty$	OC	CPU (sec)
4	$(4 + \alpha)$	2.2354E-05		1.0285E-05		7608.217903
8		5.6559E-06	1.9827	2.6057E-06	1.9808	15630.81160
16		1.4182E-06	1.9957	6.5361E-07	1.9952	26299.89527
32		3.5483E-07	1.9989	1.6355E-07	1.9987	46202.76412
4	$(3 + \alpha)$	1.5144E-04		7.4182E-05		7624.654900
8		3.8290E-05	1.9837	1.8785E-05	1.9815	15615.71326
16		9.5995E-06	1.9959	4.7115E-06	1.9954	26872.15260
32		2.4016E-06	1.9990	1.1788E-06	1.9988	49899.45439
4	$(2 + \alpha)$	8.7065E-04		4.5943E-04		8296.349491
8		2.1992E-04	1.9851	1.1627E-04	1.9824	17156.88461
16		5.5121E-05	1.9963	2.9155E-05	1.9956	29743.94537
32		1.3789E-05	1.9991	7.2944E-06	1.9989	52865.00162

In Figures 2.10 and 2.11, we display the surfaces of absolute error for Example 2.6.2 using  $\rho = (2 + \alpha)$  with uniform meshes. Figure 2.10 shows the error plots for the Nonuniform  $L1$  difference scheme (2.56)-(2.59) and Figure 2.11, for the Nonuniform

Crank-Nicolson scheme (2.74)-(2.80) with  $M_1 = M_2 = 10$ ,  $\alpha = 1.5$  at the final time  $T = 1$ .

TABLE 2.15: Temporal numerical results of the scheme (2.74)-(2.80) for Example 2.6.2 with  $h_1 = h_2 = \frac{\pi}{50}$ .

$\tau$	$\rho$	$\alpha = 1.45$		$\alpha = 1.65$		$\alpha = 1.85$	
		$\ u^\tau - U^\tau\ _\infty$	OC	$\ u^\tau - U^\tau\ _\infty$	OC	$\ u^\tau - U^\tau\ _\infty$	OC
1/5	$(4 + \alpha)$	4.0123E-04		4.3138E-04		4.5374E-04	
1/10		9.7109E-05	2.0468	1.0866E-04	1.9891	1.2251E-04	1.8890
1/20		2.2692E-05	2.0974	2.5787E-05	2.0752	3.1178E-05	1.9743
1/40		5.4076E-06	2.0691	5.9888E-06	2.1063	7.6353E-06	2.0298
1/80		1.4326E-06	1.9164	1.4205E-06	2.0759	1.8469E-06	2.0476
1/5	$(3 + \alpha)$	1.2610E-03		1.5109E-03		1.7551E-03	
1/10		2.9687E-04	2.0867	3.6747E-04	2.0397	4.6028E-04	1.9310
1/20		6.9890E-05	2.0867	8.5648E-05	2.1011	1.1463E-04	2.0055
1/40		1.7357E-05	2.0096	1.9943E-05	2.1025	2.7801E-05	2.0438
1/80		5.2216E-06	1.7329	4.9287E-06	2.0166	6.7728E-06	2.0373
1/5	$(2 + \alpha)$	2.5668E-03		3.7442E-03		5.1455E-03	
1/10		5.8008E-04	2.1457	8.5129E-04	2.1369	1.2656E-03	2.0235
1/20		2.3703E-04	1.2912	1.9295E-04	2.1414	3.0177E-04	2.0683
1/40		6.7556E-05	1.8109	4.5681E-05	2.0786	7.2050E-05	2.0664
1/80		1.5998E-05	2.0782	1.2715E-05	1.8450	1.8038E-05	1.9979

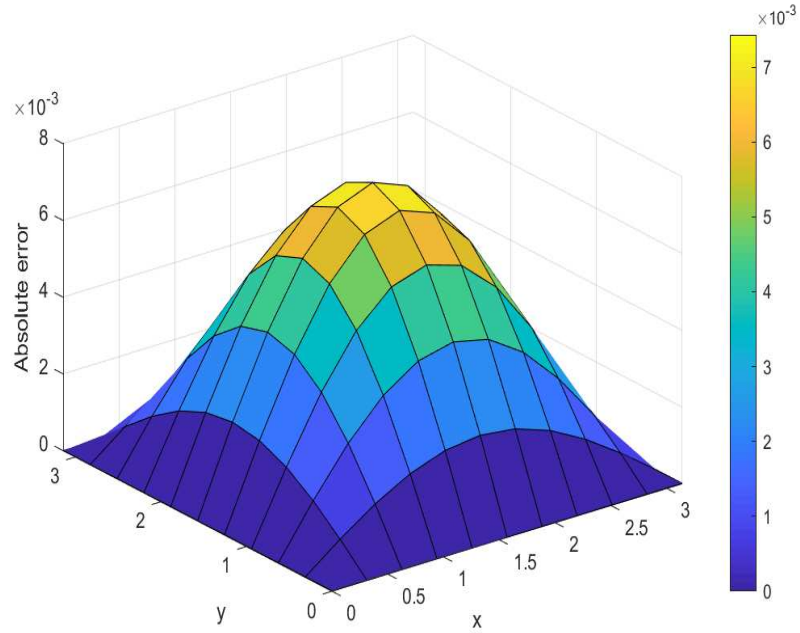


FIGURE 2.10: Absolute error surface of Example 2.6.2 for the case  $\rho = (2 + \alpha)$  using scheme (2.56)-(2.59) with  $\alpha = 1.5$ ,  $\gamma = 1$  and  $M_1 = M_2 = 10$  at  $T = 1$ .

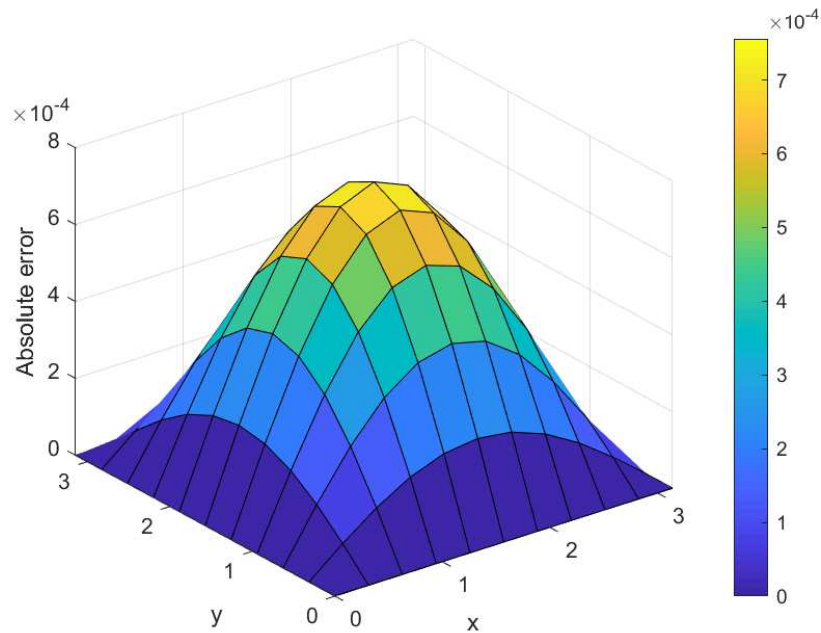


FIGURE 2.11: Absolute error surface of Example 2.6.2 for the case  $\rho = (2 + \alpha)$  using scheme (2.74)-(2.80) with  $\alpha = 1.5$ ,  $\gamma = 1$  and  $M_1 = M_2 = 10$  at  $T = 1$ .

## 2.7 Conclusion

We discussed two difference schemes on ADI approach to solve the 2D TFDWE. Two approximation methods namely Nonuniform  $L1$  method and Nonuniform Crank-Nicolson  $L1 - 2$  method were proposed to approximate the TFCD of order  $\alpha$  ( $1 < \alpha < 2$ ) in equation (2.1). The  $L1$  method is a single-term approximation method for TFCD at point  $t = t_n$  but in  $L1 - 2$  method, first we obtain  $v = u'$  from the approximation of TFCD at  $t = t_{n-\frac{1}{2}}$ ,  $n \geq 1$  then we get  $u$ . These two methods are used for the approximation of the TFCD, and central difference approximation is applied for the space derivative to get an equivalent system of equations for the considered model (2.1). The described  $L1$  and  $L1 - 2$  difference schemes have OC two in space direction and OC in time direction are  $\min(3 - \alpha, \gamma\alpha)$  and second-order, respectively. The local truncation error bounds were shown for both approximation methods. Numerical examples show that both difference schemes confirm the OC in time and space directions. Numerical algorithms have an advantage due to involvement of nonuniform mesh for solving the TFDW equation with non-smooth exact solutions having a stronger singularity at  $t = 0$ . Through provided Tables, one can conclude that the theoretical finding are validated through numerical results.

\*\*\*\*\*